

# **Investigation of crack propagation in Macro-synthetic Fiber reinforced concrete**

Suraj R. Nakhale

A Dissertation Submitted to  
Indian Institute of Technology Hyderabad  
In Partial Fulfillment of the Requirements for  
The Degree of Master of Technology



भारतीय प्रौद्योगिकी संस्थान हैदराबाद  
Indian Institute of Technology Hyderabad

Department of Civil Engineering

July, 2014

## Declaration

I declare that this written submission represents my ideas in my own words, and where others ideas or words have been included, I have adequately cited and referenced the original sources. I also declare that I have adhered to all principles of academic honesty and integrity and have not misrepresented or fabricated or falsified any idea/data/fact/source in my submission. I understand that any violation of the above will be a cause for disciplinary action by the Institute and can also evoke penal action from the sources that have thus not been properly cited, or from whom proper permission has not been taken when needed.

*Slachale*

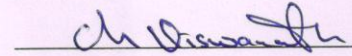
---

SURAJ R. NAKHALE

CE12M1012

## Approval Sheet

This thesis entitled **“Investigation of Crack Propagation in Macro-Synthetic Fiber Reinforced Concrete”** by Suraj R. Nakhale is approved for the degree of Master of Technology from IIT Hyderabad.

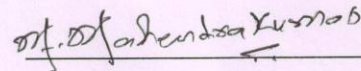


Dr. Viswanath Chinthapenta (Examiner)

Assistant Professor

Department of Mechanical & Aerospace Engineering

IIT Hyderabad

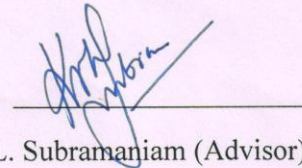


Dr. Mahendrakumar Madhavan (Examiner)

Assistant Professor

Department of Civil Engineering

IIT Hyderabad

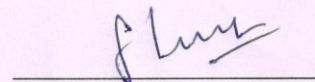


Prof. K.V.L. Subramaniam (Advisor)

Professor & Head of Department

Department of Civil Engineering

IIT Hyderabad



Dr. S. Suriya Prakash (Co-Advisor)

Assistant Professor

Department of Civil Engineering

IIT Hyderabad

## **Acknowledgements**

First and foremost, I would like to thank my guide Prof. K. V. L. Subramaniam and co-guide Dr. Suriya Prakash for his guidance and support throughout my thesis research. Project “**Investigation of crack propagation in Macro-synthetic Fiber reinforced concrete**” which helped me in doing a lot of research and I came to know about so many new things.

I would like to acknowledge all those who assisted me in the preparation and testing of specimens during my thesis research, notably GVP Bhagath singh, Mehar Babu, Sahith Gali.

Last but not the least I would like to thank my parents, who taught me the value of hard work by their own example. I would like to share this bite of happiness with my mother, father and brother. They rendered me enormous support during the whole tenure of my stay at IIT, Hyderabad.

## Abstract

The Structural Polypropylene fibre reinforced concrete (SPFRC) contains randomly distributed short discrete Polypropylene fibres which act as internal reinforcement so as to enhance the properties of the cementitious composite (concrete). The principal reason for incorporating short discrete fibres into a cement matrix is to increase the flexural tensile strength and increase the toughness and ductility and effect on properties of the fresh concrete and fracture properties of the resultant composite. These properties of SPFRC primarily depend upon length and volume of fibres used in the concrete mixture.

To determine these properties experimental work was carried out. For the study, Structural polypropylene fibres of two different lengths ( $l_f$ ) of 48 mm and 60 mm with dosage  $3\text{kg/m}^3$ ,  $4\text{kg/m}^3$  and  $6\text{kg/m}^3$  (0.33%, 0.44% and 0.66% by volume) volume fractions ( $V_f$ ) were used. The research reported in this study includes an experimental investigation to characterize selected mechanical properties of SPFRC and to study the effect of volume fraction of SPF and length of SPF on the mechanical properties.

To determine properties of concrete specimens (cubes and beams) were casted to determine the mechanical behavior such as compressive strength, flexural tensile strength. Test results showed that Structural polypropylene fiber enhanced the compressive strength and increase the toughness insignificantly. The failure of plain concrete specimens was sudden (brittle) for the flexural test. However, the concrete reinforced with Structural Polypropylene fibers showed more ductile behavior compared to the plain concrete. And also provide an interpretation for the observed tension response of fiber reinforced concrete in flexure in terms of crack propagation and toughening mechanisms in the composite.

## Nomenclature

$P_p$	peak load
$P_1$	first peak load
$\delta_p$	Net deflection at peak
$\delta_1$	first-peak loads
$F_p$	Peak Strength
$f_1$	First-Peak Strength
$P_{600}^D$	Residual load at net deflection of L/600
$f_{600}^D$	Residual Strength at net deflection of L/600
$P_{150}^D$	Residual load at net deflection of L/150
$f_{150}^D$	Residual Strength at net deflection of L/150
$T_{150}^D$	Area under the load vs. net deflection curve 0 to L/150
$R_{T150}^D$	Equivalent flexural strength
$T_{JSCE}$	Toughness
$F_{JSCE}$	Toughness factor
<b>CMOD</b>	Crack mouth opening displacement
<b>LOP</b>	Limit of proportionality
$F_L$	load corresponding to LOP
$f_{ct,L}^f$	Strength corresponding to LOP
$F_i$	load corresponding to with CMOD = CMOD <sub>j</sub> or $\delta = \delta_i$ (I = 1,2,3,4)
$f_{R,j}$	Residual flexural Tensile Strength corresponding with CMOD = CMOD <sub>j</sub> or $\delta = \delta$ (i= 1,2,3,4)
<b>CTOD</b>	Crack Tip opening displacement
$P_{1f}$	First crack load
$f_{1f}$	First crack strength
$U_1$	Areas under load–CTOD <sub>m</sub> curve for CTOD <sub>net</sub> intervals equal to 0–0.6 mm
$U_2$	Areas under load–CTOD <sub>m</sub> curve for CTOD <sub>net</sub> intervals equal to 0.6-3 mm
$f_{eq(0-0.6)}$	equivalent flexural strength
$f_{eq(0.6-3)}$	equivalent flexural strength
$D_0$	Ductility indexes
$D_1$	Ductility indexes

## List of figures

- Fig.2.1** The composite stress-strain curves for fiber-reinforced brittle matrix
- Fig.2.2** Strain hardening response of polypropylene fiber composites
- Fig.2.3** Effect of steel fiber shape on the load response in flexure
- Fig.2.4** Various types of synthetic fibers tested in the present study
- Fig.2.5** Comparison of absorbed energies from pullout tests for various fiber types.
- Fig.2.6** Load–deflection curves for HE 60 at 30, 40 and 50 kg/m<sup>3</sup> dosage rates and for S 4.6 and S 5.3 at 4.6 and 5.3 kg/m<sup>3</sup> dosage rates.
- Fig.2.7** Schematic diagram of a Suitable Apparatus for Flexure Test of Concrete by Third-Point Loading Method.
- Fig.2.8** Standard Load-Displacement Curves per ASTM C1609 -10
- Fig.2.9** Important Characteristics of the Load-Deflection Curve
- Fig.2.10** Definition of Toughness Indices in Terms of Multiples of First-Crack Deflection and Elastic- Perfectly Plastic Material Behaviour.
- Fig.2.11** Definitions of JSCE Toughness and Toughness Factor
- Fig.2.12** Schematic diagram of the UNI 11309 four-point bending test setup
- Fig.2.13** (a) Basic concrete load-CMOD diagram showing CMOD<sub>0</sub>; (b) Load–CTOD diagram: U<sub>1</sub> e U<sub>2</sub> determination
- Fig.2.14** Typical arrangement of measuring CMOD
- Fig.2.15** Load-CMOD and F<sub>j</sub> (j=1,2,3,4)
- Fig.2.16** PCS analysis on a FRC beam
- Fig.3.1** FibreTuff™ Monofilament structural polypropylene fiber
- Fig.3.2** Test setup as per ASTM C 1609
- Fig.3.3** Test setup as per EN 14651-2005
- Fig.3.4** Test setup of DIC
- Fig.4.1** Effect of volume fraction on slump
- Fig.4.2** Failure of beam
- Fig.4.3** Load vs Displacement curve for control, 3kg/m<sup>3</sup>, 4kg/m<sup>3</sup> and 6kg/m<sup>3</sup>
- Fig.4.4** Comparison typical specimen of Load vs Displacement curve for control and 3,4 and 6kg/m<sup>3</sup>

- Fig.4.5** Comparison typical specimen of Peak Load for PC and 3, 4 and 6kg/m<sup>3</sup>
- Fig.4.6** Load vs CMOD curve for control, 3kg/m<sup>3</sup>, 4kg/m<sup>3</sup> and 6kg/m<sup>3</sup>
- Fig.4.7** Comparison of typical specimen of Load vs CMOD curve for PC and 3, 4 and 6kg/m<sup>3</sup>
- Fig.4.8** Grid of 1 inch X 1 inch for fiber distribution
- Fig.4.9** Load response of a specimen with 6kg/m<sup>3</sup> and  $\epsilon_{xx}$  at distinct points in the load response on the load response.
- Fig.4.10** Location of lines
- Fig.4.11**  $\epsilon_{xx}$  along line one for control, 4kg/m<sup>3</sup> and 6kg/m<sup>3</sup>
- Fig.4.12** Distinct point on the load response of specimen at pre peak, around peak and post peak
- Fig.4.13** Strain at pre peak, around peak and post peak

## List of tables

- Table 2.1** Typical Properties of Fibers
- Table 2.2** Properties of various types of polypropylene fiber
- Table 3.1** Summary of weight proportion of the various mixes
- Table 4.1** Properties of the fresh concrete measured during the casting of the different sets of specimens.
- Table 4.2** Compressive strength for cube
- Table 4.3** Test results for all specimens tested as per ASTM C-1609
- Table 4.4** flexural toughness indices using ASTM C-1018
- Table 4.5** flexural toughness indices using JSCE SF 24
- Table 4.6** Stress at LOP and Residual Strength and using EN 14651-2005
- Table 4.7** Location of lines
- Table 4.8** Hinge length
- Table 4.9** Load at lines



# Contents

Declaration.....	ii
Approval Sheet .....	iii
Acknowledgements.....	iv
Abstract.....	v
<b>Nomenclature .....</b>	<b>vi</b>
<b>List of figures.....</b>	<b>vii</b>
<b>List of tables .....</b>	<b>viii</b>
<b>1 Introduction.....</b>	<b>1</b>
1.1 Objectives .....	2
1.2 Organization of thesis .....	3
<b>2 Review of Literature .....</b>	<b>4</b>
2.1 Steel Fibers .....	7
2.2 Polypropylene Fibers .....	8
2.3 Macrosynthetic Polypropylene fiber.....	9
2.4 Review of standardize test method .....	12
2.4.1 ASTM 1609.....	13
2.4.2 ASTM 1018.....	15
2.4.3 JSCE SF4.....	16
2.4.4 UNI 11039-2.....	17
2.4.5 EN 14561.....	19
<b>3 Materials and Methods.....</b>	<b>23</b>
3.1 Cement.....	23
3.2 Fly Ash .....	23
3.3 Aggregates .....	23
3.4 Polypropylene fiber .....	24
3.5 Admixture .....	24
3.6 Experimental program and Mix Proportions .....	24
3.6.1 Casting and Curing of Specimens .....	25
3.7 Test Methods .....	26
3.7.1 Slump .....	26

3.7.2	Compression Strength Testing .....	26
3.7.3	Flexural Test.....	27
3.7.4	Digital Image Correlation -DIC (For notch beam).....	29
<b>4</b>	<b>Result and Discussion .....</b>	<b>30</b>
4.1	Introduction.....	30
4.2	Workability of fresh SPFRC.....	30
4.3	Compressive strength.....	32
4.4	Flexural test results as per ASTM C 1609 (For unnotch beam) .....	33
4.5	Flexural test results as per EN 14651-2005 (For notch beam) .....	39
4.6	Fiber distribution .....	41
4.7	DIC test result .....	42
4.8	Analysis of Results .....	48
<b>5</b>	<b>Summary of finding and Future Work.....</b>	<b>51</b>
	<b>References.....</b>	<b>53</b>

# Chapter 1

## Introduction

The addition of the fibres to concrete has been shown to enhance the toughness of concrete. The ability of fibre-reinforced concrete composites to absorb energy has long been recognized as one of the most important benefits of the incorporation of fibres in plain concrete. Fibers bridge a crack and provide resistance to crack opening which imparts post-cracking ductility to the cementitious composite which would otherwise fail in a brittle manner.

A concrete beam containing fibres suffers damage by gradual development of single or multiple cracks with increasing deflection, but retains some degree of structural integrity and post-crack resistance even under considerable deflection. A similar beam without fibres fails suddenly at a small deflection by separation into two pieces. The toughening effect is the result of several types of fiber/matrix interactions, which leads to energy absorption in the fiber-bridging zone of a fiber-reinforced concrete (FRC). These processes include fiber bridging, fiber debonding, fiber pullout (sliding) and fiber rupture as a crack propagates across a fiber through the matrix [1]

There are many kinds of fibers, both metallic and polymeric, which have been used in concrete to improve specific engineering properties of the material. Steel fibres are used in a wide range of structural applications, in general, when the control of concrete cracking is important such as industrial pavements [2,3], precast structural elements [4] and tunnel linings [5]. Steel fibers have high elastic modulus and stiffness and produce improvements in compressive strength and toughness of concrete [6]. Improvements in flexural strength of the material are also obtained by the use of steel fibres in concrete. Increase in flexural strength is achieved with increasing fiber aspect ratio (length to diameter ratio) and fiber volume fraction; significant improvements are obtained at high volume fractions [7]. In general, addition of steel fibers influences the compressive strain at ultimate load and

ductility in flexure more significantly than the improvements in strength [8]. Steel fibers, however, increase structure weight of concrete and exhibit balling effect during mixing, which lowers the workability of the mix. In addition, steel fibers easily basset and rust, and it also has the problem of conductive electric and magnetic fields.

Synthetic fibres are usually smaller than steel fibres and are most typically used in industrial pavements to reduce the cracking induced by shrinkage. Polypropylene fibers have good ductility, fineness, and dispersion so they can restrain the plastic cracks [9]. Synthetic fibres are mainly effective in reducing crack formation, particularly at an early stage of the cast and in severe weather conditions (e.g. in dry climatic zones), when hygrometric shrinkage brings along some weak tensile stress which is yet too high for the fresh mixture to withstand.

Improvements are being made to optimize fibers to suit applications. Recently, macro-synthetic fibres have been produced with the aim of substituting steel fibres in structural applications. There has been a growing interest on synthetic fibres, owing to some substantial advantages over metallic ones, such as strong chemical stability in alkaline and generally aggressive environments, exemption from oxidation, lightness and, in turn, convenient stocking and handling, a-toxicity and electromagnetic transparency. This latter aspect is relevant, for instance, when either dealing with special equipment (ranging from mobile phones to CT diagnostics) or in industrial buildings wherein, say, automated toll collection booths employing electromagnetic vehicle detectors are planned. The availability of a structural synthetic fibre, capable of contributing to the load carrying capacity of an element while increasing its toughness and durability at a reasonable cost, is an important asset for an improved building technology. The knowledge on the mechanical behaviour of concretes reinforced with these fibres is still limited.

## **1.1 Objectives**

The broad objective of the work reported in this thesis is to investigate the influence of macro synthetic fibers on the mechanical behaviour of concrete. Specific objectives of the thesis include

1. To evaluate the influence of macro-synthetic polypropylene fibers on the workability and compressive strength of concrete.
2. To evaluate the influence of macro-synthetic polypropylene fibers on the toughness and ductility of concrete.

3. To provide an interpretation for the observed tension response of fiber reinforced concrete in flexure in terms of crack propagation and toughening mechanisms in the composite.

## **1.2 Organization of thesis**

This thesis is organized in four chapters. Description of content of each chapter is given below.

### **Chapter 2**

A review of literature on the influence of fibers on the mechanical properties and tension response of concrete is presented. The influence of fiber type and volume fraction on the tensile response of concrete are summarized.

### **Chapter 3**

Details of the experimental program to investigate the tensile behaviour of macro synthetic fiber reinforced concrete are presented in this chapter. The materials and test methods used in the experimental test program are described.

### **Chapter 4**

Results of the test program into the fresh and hardened properties of concrete are presented.

### **Chapter 5**

The results of the experimental investigation reveals into summary of finding and future work.

# Chapter 2

## Review of Literature

Fibers have been used as discrete randomly distributed reinforcement to strengthen a material weak in tension. Fibers have been shown to improve the toughness and the post crack ductility in tension, which is achieved by the reinforcement effect across a crack in the material matrix. The use of fibers results in an enhancement in the load carrying ability which is achieved due to stress transfer after cracking. The earliest documented use of fibers has been the incorporation of chopped hay and camel hair in adobe bricks by the Egyptians. Since then different types of fibers have been developed, which can broadly be classified as metallic, synthetic, glass, and mineral. Properties of the different fibers commonly available today are listed in Table 2.1.

Table 2.1: Typical Properties of Fibers

<b>Fiber</b>	<b>Diameter</b>	<b>Specific gravity</b>	<b>Tensile strength</b>	<b>Elastic Modulus</b>	<b>Fracture strain</b>
	<b>(<math>\mu\text{m}</math>)</b>		<b>(GPa)</b>	<b>(GPa)</b>	<b>(%)</b>
Steel	5-500	7.84	0.5-2.0	210	0.5-3.5
Glass	9-15	2.6	2.0-4.0	70-80	2.0-3.5
Fabrilated Polypropylene	20-200	0.9	0.5-0.75	5-77	8.0
Cellulose		1.2	0.3-0.5	10	
Carbon (high strength)	9	1.9	2.6	230	1
Cement matrix (For comparison)		2.5	$3.7 \times 10^3$	10-45	0.02

Fiber volume content is the primary variable which influences the response of the fiber reinforced composite in tension as shown in Figure 2.1. For small volume fraction, after first crack, there is drop in the load. There are a small number of fibers bridging the crack that

sustain the load. The capacity provided by the number of fibers crossing the crack is significantly less than the first crack load and load carrying capacity decreases rapidly with increasing deformation. For intermediate volume fraction, after the drop in load associated with the formation of a crack, the load carrying capacity provided by the fibers produces a progressive yet gradual decrease in the load carrying capacity. For high volume fraction, after first crack, there are a large number of fibers bridging the crack and the resistance to crack opening provided by the fibers is larger than the first crack load. As the load increases, more cracks form along the length of specimen.

The observed load response at the different volume fractions is associated with the pullout response of steel fibers from the concrete matrix averaged over the crack. The mechanical behaviour of the FRC are influenced by reinforcing mechanisms or the ability of the fibers to transfer stress across the crack. In short randomly distributed fibers at low and intermediate fiber volume fractions (typically up to 2%) the contribution of fibers is after strain localization, which occurs close to the peak tensile load. The tensile strength in these cases is comparable to that of the unreinforced matrix. The strain softening is influenced by the cracking closing pressure provided by the fibers as a function of the crack opening displacement. The toughening provided fibers depends upon the pull out resistance of the fibers embedded in the matrix. During crack propagation, debonding and sliding contribute significantly to the pull out resistance of the fibers and hence to the total energy consumption when a large crack develops in the matrix. Fiber breakage has not been considered to contribute significantly to the energy dissipated during crack propagation in FRC [10]. Several fracture based formulations which consider the debonding behaviour of fibers from the cementitious matrix have been proposed [10].

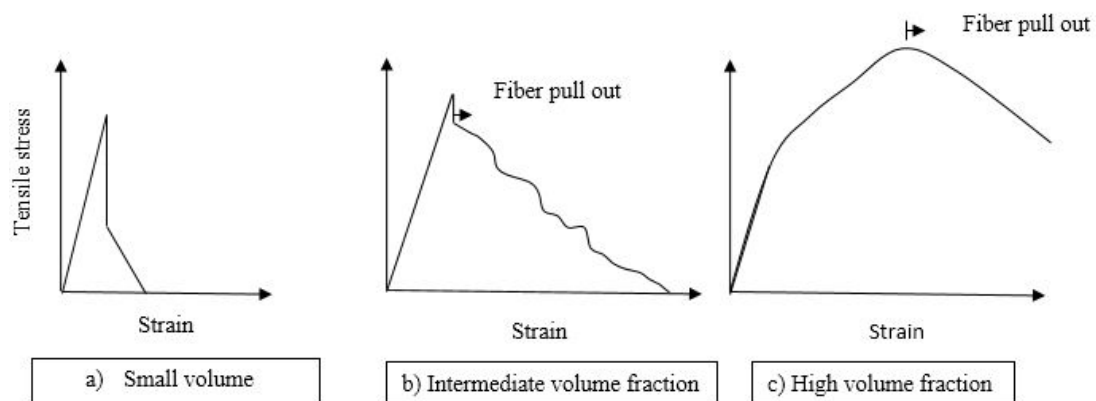


**Figure 2.1: The composite stress-strain curves for fiber-reinforced brittle matrix**

At higher volume fractions, which are usually achieved using special processing techniques, the pre-peak behaviour is fundamentally altered due to stabilization of micro cracking in the matrix. A uniform distribution of micro cracks in the matrix leads to significant enhancement in the strain capacity of the matrix. The load response of such composites exhibits strain hardening response as show in Figure 2.2. There is a point in the load response identified as the bend-over-point (BOP) where the matrix contribution to the tensile load response reaches a maximum. The load response following the BOP is characterized by multiple cracking in the matrix. In this stage the incremental loading of the fibers at the location of the crack is transferred to the matrix through the interfacial bond, which results in a build-up of tensile stress in the matrix. More cracks are produced in the matrix when the tensile stress in matrix reaches the tensile strength of the matrix. Mechanistic and fracture based approaches which consider fiber-matrix interaction in high volume composites where the localization of crack is suppressed is very complex and is still developing.

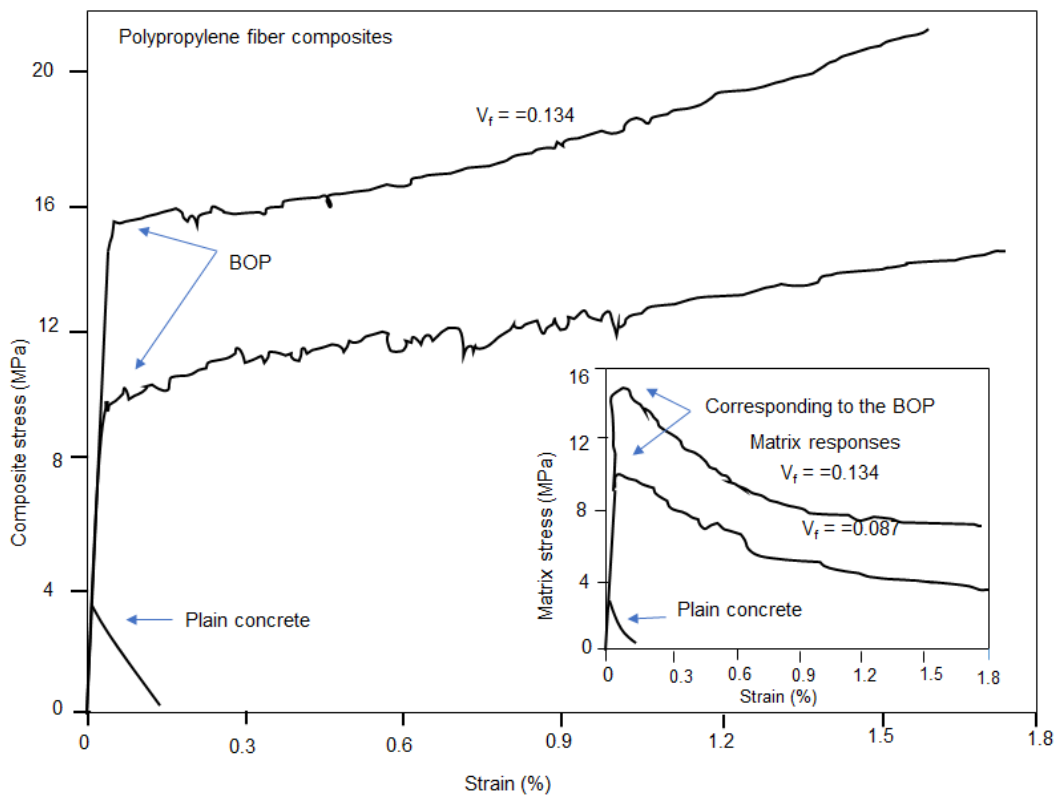


**Figure 2.2: Strain hardening response of polypropylene fiber composites**



The available literature on the behaviour of steel and synthetic fibers is reviewed

## **2.1 Steel Fibers**

Steel fibers Steel fibers have a relatively high strength and modulus and are available in aspect ratios ranging from 20 to 100 and length ranging from 6.4mm to 75mm. The process of manufacture varies from cut sheets, cold drawn wires or hot melt extraction and are available in different cross-sections and shapes depending on the method of manufacture and use.

While steel fibers improve the strength of concrete under all load actions, their effectiveness in improving strength varies among compression, tension and flexure. There is an insignificant change in the ultimate compressive strength upon the addition of steel fibers; There is an increase of up to 15 percent for volume of fibers up to 1.5 percent by volume [11,12]. There is a significant improvement in strength in tension with an increase of the order of 30 to 40 percent reported for the addition of 1.5 percent by volume of fibers in mortar or concrete [12,13]. Strength data [11] shows that the flexural strength of SFRC is about 50 to 70 percent more than that of the unreinforced concrete matrix in the normal third-point bending test [14, 15].

The ability of steel fibers to serve as reinforcement is determined by the resistance of the fibers to pullout from the matrix resulting from the breakdown of the fiber-matrix interfacial bond [10]. Improvements in ductility depend on the type and volume percentage of fibers present [16,17]. In conventionally mixed SFRC, high aspect ratio fibers are more effective in improving the post-peak performance because of their high resistance to pullout from the matrix. However, at high aspect ratio there is a potential for balling of the fibers during mixing [8]. Techniques such as enlarging or hooking of ends, roughening their surface texture, or crimping to produce a wavy rather than straight fiber profile allow for retaining high pullout resistance while reducing fiber aspect ratio. These types are more effective than equivalent straight uniform fibers of the same length and diameter. Consequently, the amount of these fibers required to achieve a given level of improvement in strength and ductility is usually less than the amount of equivalent straight uniform fibers [18,19].

The fiber pullout behaviour is influenced by the type of fiber as seen in the load response obtained from steel fiber reinforced concrete with 50 kg/m<sup>3</sup> fibers in Figure 2.3. For hooked

end steel fiber, after first crack, there is drop but that drop is less than the other two fibers, deformed end fiber and corrugated fiber. For deformed end fiber and corrugated fiber, after first crack .there is a continuous decrease in the load carrying capacity with increasing deformation. Hooked end fibers, which provide the highest pullout resistance from the matrix provide the highest load carrying capacity with increasing deformation after crack formation.

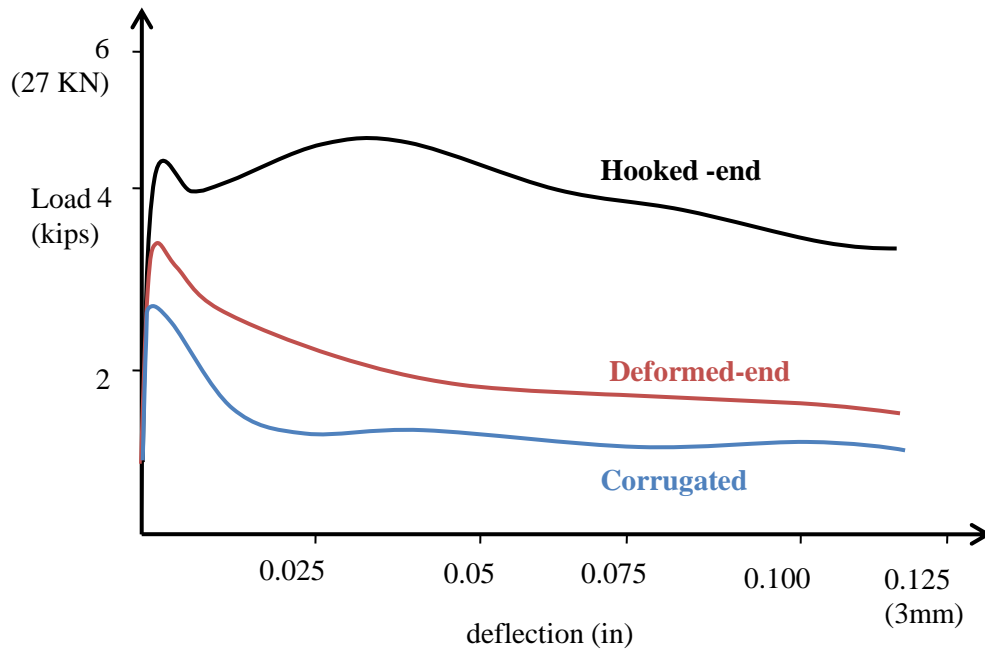


**Figure 2.3: Effect of steel fiber shape on the load response in flexure**

Improvements in post-crack ductility under tension result in significant improvements in flexural response. Ductile behavior of the SFRC on the tension side of a beam alters the normally elastic distribution of stress and strain over the member depth. The altered stress distribution is essentially plastic in the tension zone and elastic in the compression zone, resulting in a shift of the neutral axis toward the compression zone [20].

## 2.2 Polypropylene Fibers

Most commercial applications of polypropylene fibers have used low volume percentage (0.1 percent), monofilament or fibrillated fibers (in the case of polypropylene). Typical properties of monofilament and fibrillated polypropylene fibers is given in Table 2.2.

Table 2.2: Properties of various types of polypropylene fiber

Fiber type	Length	Diameter	Tensile strength	Modulus of elasticity	Specific Surface	Density
	(mm)	(mm)	(MPa)	(MPa)	(m <sup>2</sup> /kg)	(kg/cm <sup>3</sup> )
Monofilament	30-50	0.30-0.50	547-658	3.50-7.50	91	0.9
Microfilament	12-20	0.05-0.20	330-414	3.70-5.50	225	0.91
Fibrillated	19-40	0.20-0.30	500-750	5.00-10.00	58	0.95

These use of these fibers have been restricted to nonstructural and non-primary load bearing members.

At typical dosages usually employed in the construction industry there is a marginal improvement in the mechanical properties of concrete.

At dosages considered by the industry, of 1.2 kg/m<sup>3</sup>, PP fibers have been shown to influence the fracture behaviour; the influence of the fibres was especially felt in the tail of the P-d curve, showing a wider softening branch in the case of the FRC mixes, which corresponds to a more ductile behavior of the concrete. The effect of the fibre is more remarkable in the case of the low strength concrete, where the stresses in the cohesive zone are lower, and the bridge effect of the fibre has a greater effect due to the higher level of deformation. It was shown that the fibres with the highest elongation and lowest strength (i.e. the most ductile fibres) presented the highest values of fracture energy. In the case of high strength concrete the higher level of the cohesive stresses mitigates the bridge effect of the fibres. In low- and normal-strength concrete the main mechanism of failure of the fibres was by pull-out while in high strength concrete it was due to fiber breakage [21].

### 2.3 Macrosynthetic Polypropylene fiber

Structural synthetic fibers are available in different geometries and shapes as shown in Figure 2.4. The energy absorption capacities from pullout tests on the different shape synthetic fiber obtained from pullout tests are shown in Figure 2.5 [22,23]. Test results indicate that the crimped-shape structural synthetic fibers exhibit the highest energy absorption capacity.

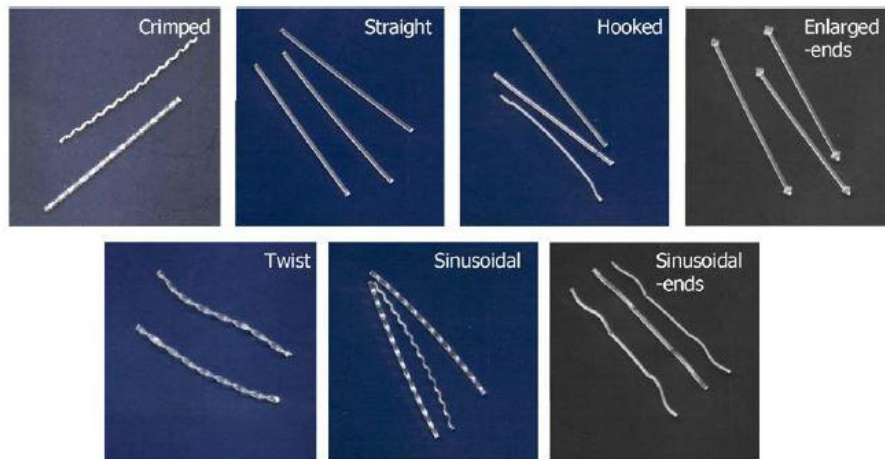


**Figure 2.4: Various types of synthetic fibers tested in the present study**

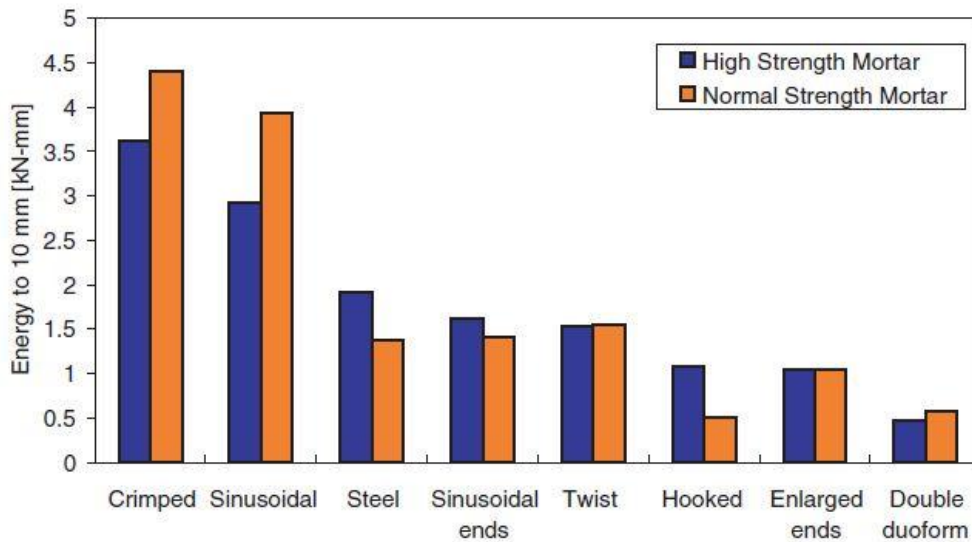


**Figure 2.5: Comparison of absorbed energies from pullout tests for various fiber types.**

A comparison of the load response in flexure between hooked end steel fibers and synthetic fibers is shown in Figure 2.6. Data obtained from M.N. Soutsos et al T.T. Le and A.P. Lampropoulos are plotted in the Figure 2.6. Steel fibers at dosages up to  $60 \text{ kg/m}^3$ , show in a drop in load immediately after formation of the crack, followed by a gradual decrease in load carrying capacity. In case of synthetic fiber, at fiber dosage rate  $4.6 \text{ kg/m}^3$ , there is sudden drop (that drop decrease in fiber dosage rate  $5.3 \text{ kg/m}^3$ ), after first crack, there is continuously decreasing load and increasing the deflection (slowly fiber pull out start from the matrix).

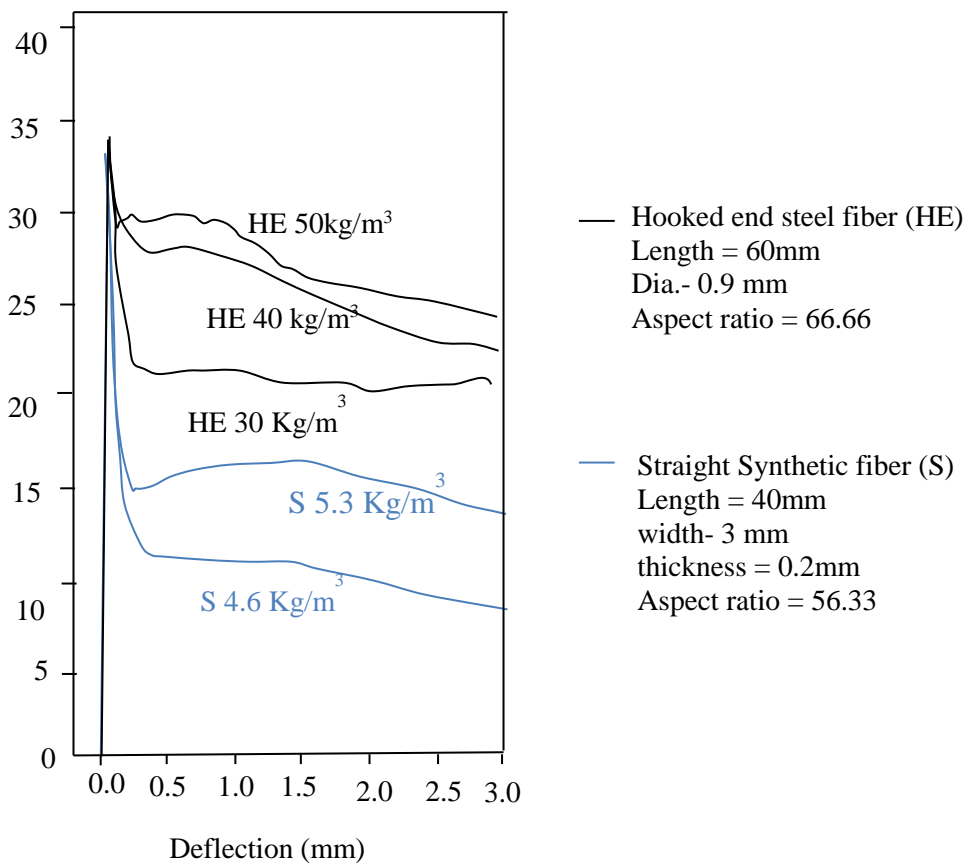


**Figure 2.6: Load–deflection curves for HE 60 at 30, 40 and 50 kg/m<sup>3</sup> dosage rates and for S 4.6 and S 5.3 at 4.6 and 5.3 kg/m<sup>3</sup> dosage rates.**

A comparative study on the mechanical behavior and fracture properties and fracture behavior of concrete containing steel fiber and micro-polypropylene fiber (19mm length) was published by Bencardino et al (year). It was found that while steel fibers had an insignificant influence on the compressive strength of concrete, Polypropylene fibers reduced the compressive strength about 25% and 35% at 1% and 2% fiber volumes, respectively. This was attributed to the low modulus of elasticity of the polypropylene fibers and insufficient dispersion of the fibers in the mixture. The elastic modulus of steel fibers were also shown to influence the fracture properties and behaviour obtained using notched beams tested in three-point bending configuration. The equivalent flexural strength values of SFRC are much higher than the strength at the limit of proportionality, while for polypropylene fibers, the reverse is true. Steel fibers produced an increase in the peak load with increase in the steel fiber volume content when compared with ordinary concrete. The polypropylene fiber reinforced concrete specimens were able to retain peak load values similar to those recorded for the control specimens at 1% fiber volume content. However, at the 2% fiber volume content, these specimens showed a substantial decrease in peak flexural loads compared to those of the control. After reaching the peak load, all the PFRC

specimens showed sudden drop in load, about 67% and 40% of the peak load for fiber volume contents of 1% and 2%, respectively. The residual loads after the load drop remained constant with increasing deflection, up to the end of the test. Macro synthetic fibers were shown to be significantly less effective than the hooked end steel fibers in increasing the fracture energy.

However, the low modulus polypropylene fibers were shown to give as much ductility as the steel fibers.

In their study involving a comparison of hooked end steel fibers and macro synthetic fibers (slightly coiled Polyolefinic, hooked Polystyrene, flat polymeric mix), Buratti et al. (2011) also showed that the residual strength for steel fibers are higher when compare to macro synthetic fibers from notched concrete beams tested in three-point configuration. At volume fractions in the range of 0.2-0.5%, the residual strength was found to increase with an increase the fiber content. The addition of fibres, both steel and macro-synthetic, to the concrete increased its toughness from 5 to 10 times. The results of the experimental investigation revealed that considering the variability of results, the mean values of residual strengths at different CMOD opening normalized to its corresponding flexural strength indicate a significant improvement in the performance of the steel fibres when compared with synthetic fibres. If the characteristic residual strengths, which are obtained as the 5 percentile values are used, the benefit given by the steel fibres is reduced. A direct correlation between the statistical distribution of fibers in the crack plane and the residual strength values is also shown for the macro synthetic fibers.

## **2.4 Review of standardize test method**

Standardized test methods for quantifying improvements in material behaviour and obtaining specific material properties have been developed. In these tests material parameters which quantify ductility and toughness of the material are obtained from measured load response. The quantities derived from these tests allow for comparison of material behaviour. Standard test procedures for evaluating the response of FRC are available in ASTM 1609, UNI 11039-2, ASTM 1018, EN 14651 and JSCE SF 24. Additionally, researchers have proposed methods for obtaining fracture or material parameters from the measured test response from the standardized test procedures. The test procedures and the different data reduction procedures are reviewed in this section.

### 2.4.1 ASTM 1609

ASTM C1609/C1609 M-05 provides a standardized test procedure to establish the flexural toughness, the flexural strength and the residual strength factors of the fiber reinforced concrete from the load-deflection curve through testing of a simply supported beam under third-point loading. The loading and support system capable of applying third point loading the specimen without eccentricity or torque in accordance with ASTM C78-02 is shown in Figure 2.7. Test is performed measuring the applied load and the beam net deflection (i.e. the absolute mid-span deflection minus the support deflection) at a constant deflection rate. The beam midpoint deflection between the tension face of the beam is measured in relation to the neutral axis of the beam at its support.

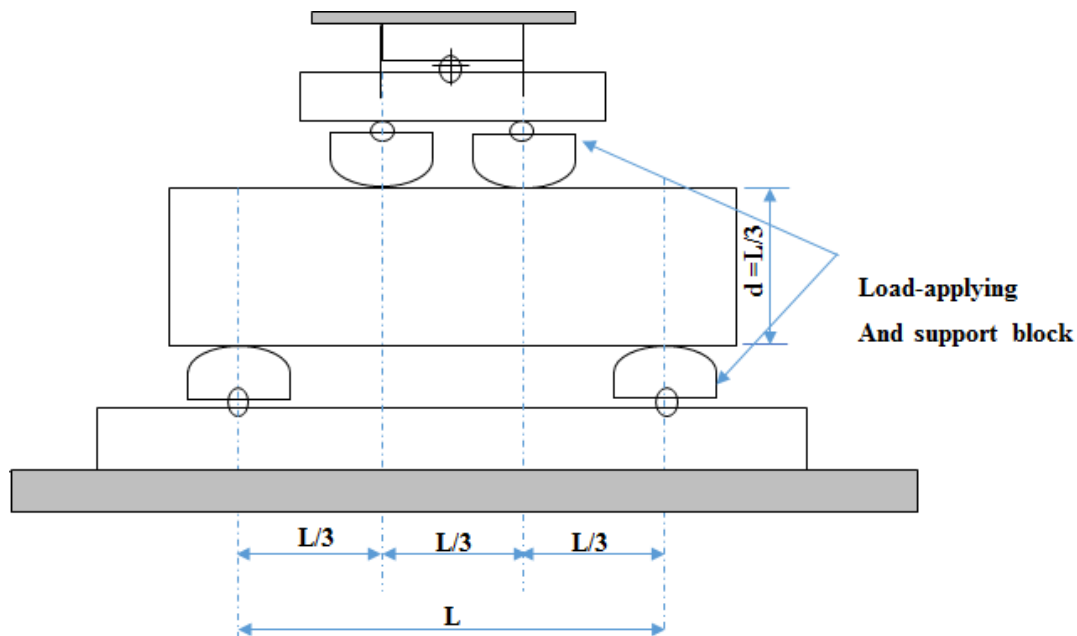


**Figure 2.7: Schematic diagram of a Suitable Apparatus for Flexure Test of Concrete by Third-Point Loading Method.**

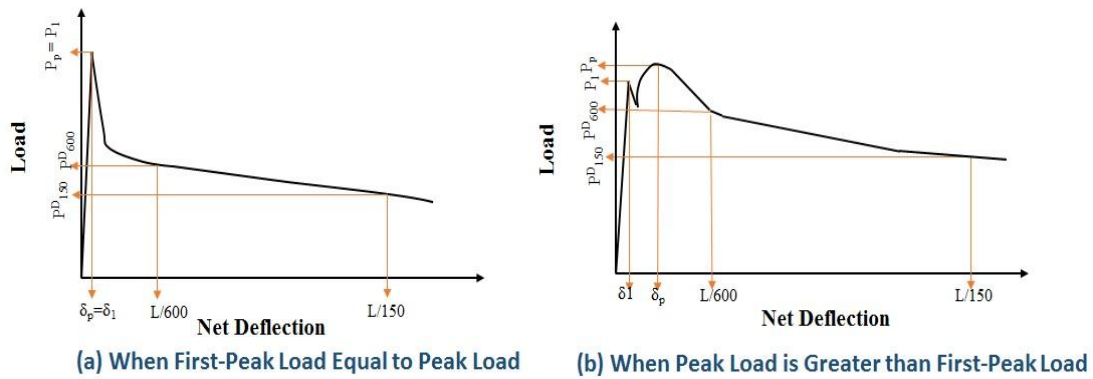
First peak deflection, toughness and Equivalent flexural strength are derived from the measured response. The standard load-displacement behaviours of fiber reinforced concrete beams are shown in Figure 2.8. The peak load is determined as that value of load corresponding to the point on the load-deflection curve that corresponds to the greatest value of load obtained prior to reaching the end-point deflection. The first-peak load is defined as that value of load corresponding to the first point on the load-deflection curve where the slope is zero, that is, the load is a local maximum value. In specimens, which

exhibit an increase in load after the load drop produced by cracking, the first peak load is the distinctive point in the load response associated with load drop as shown in Figure 2.8. Strength corresponding to each peak load,  $f_p$  is determined following formula for modulus of rupture

$$f = \frac{PL}{bd^2} \quad (2)$$

First-peak deflection for third-point loading is estimated assuming linear-elastic behavior up to first peak from the equation.

$$\delta_1 = \frac{23P_1L^3}{1296EI} \left[ 1 + \frac{216d^2(1+\mu)}{115L^2} \right] \quad (1)$$



**Figure 2.8: Standard Load-Displacement Curves per ASTM C1609 -10**

The residual strengths,  $f^D_{600}$  and  $f^D_{150}$  are determined from the residual load values,  $P^D_{600}$  and  $P^D_{150}$  corresponding to net deflection values of  $1/600$  and  $1/150$  of the span length.

Toughness  $T^D_{150}$  is determined as the total area under the load-deflection curve up to a net deflection of  $1/150$  of the span length. The equivalent flexural strength ratio,  $R^D_{T,150}$  is determined according to Eq. 3 using the first-peak strength determined and the toughness determined. Record the number rounded to the nearest 0.5 % as equivalent flexural strength ratio,  $R^D_{T,150}$  as appropriate for the specimen depth.

$$R^D_{T,150} = \frac{150T^D_{150}}{f_1bd^2} 100\% \quad (3)$$



## 2.4.2 ASTM 1018

ASTM C1018 provides standardized measures of toughness indices taken as the area under the load-deflection curve up to the first crack to area under the load-deflection curve up to certain specified deflection from the load-deflection curves of specimens. From the load-deflection curves obtained using the loading procedure specified in ASTM 1609, toughness indices are calculated at three level of deflection  $3\delta$ ,  $5.5\delta$  and  $10.5\delta$ , corresponding to 3, 5.5 and 10.5 times the deflection at first crack, Deflection values greater than  $10.5\delta$  can also be chosen for composite that can carry considerable loads at large deflection Figure 2.9. The three suggested indices called  $I_5$ ,  $I_{10}$  and  $I_{20}$  are defined by following equations.

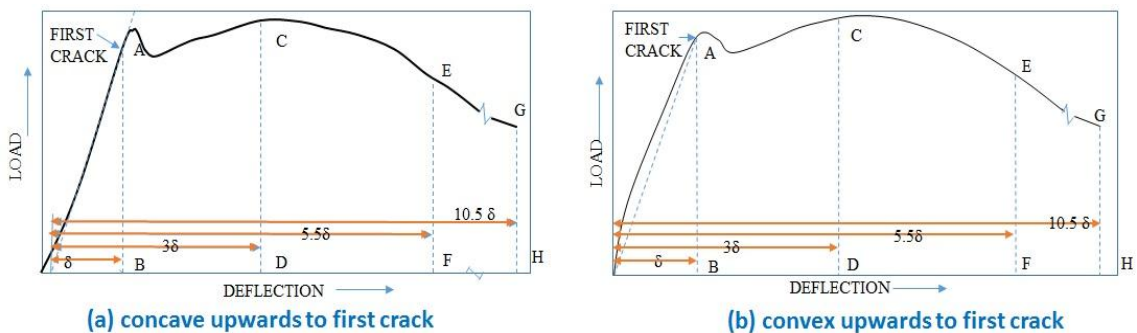


Figure 2.9: Important Characteristics of the Load-Deflection Curve

The deflection values of  $3\delta$ ,  $5.5\delta$  and  $10.5\delta$  were chosen using elastic perfectly plastic behavior as the datum as shown in Figure 2.10. Residual loads at specified deflections, the corresponding residual strengths and determination of specimen toughness based on the area under the load-deflection curve up to a prescribed deflection and the corresponding equivalent flexural strength ratio are also obtained.

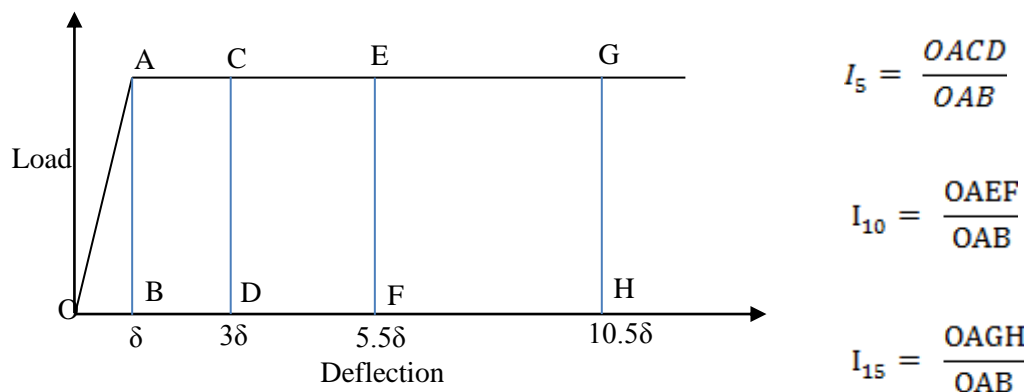


Figure 2.10: Definition of Toughness Indices in Terms of Multiples of First-Crack Deflection and Elastic- Perfectly Plastic Material Behaviour.

$$I_5 = \frac{\text{Area under the load – deflection curve up to } 3\delta}{\text{Area under the load – deflection curve up to } \delta}$$

$$I_{10} = \frac{\text{Area under the load – deflection curve up to } 5.5\delta}{\text{Area under the load – deflection curve up to } \delta}$$

$$I_{20} = \frac{\text{Area under the load – deflection curve up to } 10.5\delta}{\text{Area under the load – deflection curve up to } \delta}$$

### 2.4.3 JSCE SF4

Ductility is commonly measured using the Japanese standard test method JSCE-SF4, which used beams in a third-point loading arrangements. The JSCE SF 24 provides a measure of flexural toughness from the measured load-deflection response as shown in Figure 2.11. The value of toughness,  $T_{JSCE}$  is determined as the area under the load-deflection curve up to a deflection equal to span/150. Toughness factor,  $F_{JSCE}$  is derived from the value of toughness.  $F_{JSCE}$  has the unit of stress such that its value indicates, in a way, the post-matrix cracking residual strength of the material when loaded to a deflection of span/150. The chosen deflection of span/150 for its calculation is purely arbitrary and is not based on serviceability considerations.

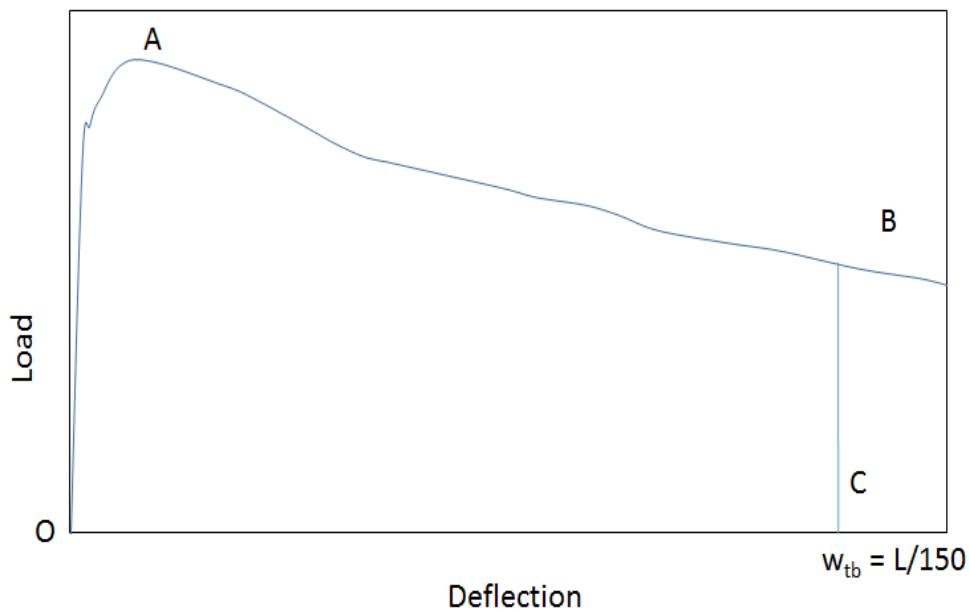


Figure 2.11: Definitions of JSCE Toughness and Toughness Factor

## Toughness

$$T_{JSCE} = AREA_{OAEFO}$$

## Toughness factor

$$F_{JSCE} = \frac{T_{JSCE} L}{BH^2 w_{tb}}$$

The equivalent flexural strength as defined by the JSCE-SF4 for a deflection of 3 mm, the Re.3 value, a measure of the ductility, is the average load applied as the beam defects to 3 mm expressed as a ratio of the load to first crack. This measure is also known as the equivalent flexural strength as denoted as  $f_{e,3}$ , has been calculated as

$$f_{e,3} = \frac{P_{mean,150} \times l}{bd^2}$$

Where  $P_{mean,150}$  is the area under the load-deflection curve divided by the limit deflection of 3 mm and  $l$ ,  $b$  and  $d$  are the span, width and depth of the prism, respectively (i.e. 450 mm, 150 mm and 150 mm, respectively).

### 2.4.4 UNI 11039-2

UNI 11039-2 bending test is a four-point loading test on a prismatic beam. UNI test specifically prescribes the specimen absolute dimensions; the UNI test employs a notched beam with a specimen which is 150 mm deep, 150 mm wide and the span length is 450 mm. The notch is sawed at mid-span with a depth,  $a_0$  equal to 0.3 times the overall specimen depth ( $a_0 = d/3$ ). The test is performed measuring the load,  $P$  and the Crack Tip Opening Displacement (CTOD), while increasing the Crack Mouth Opening Displacement (CMOD) at a constant rate equal to  $0.05 \pm 0.01$  mm/min. A schematic diagram of the UNI test setup is shown in Figure 2.12.

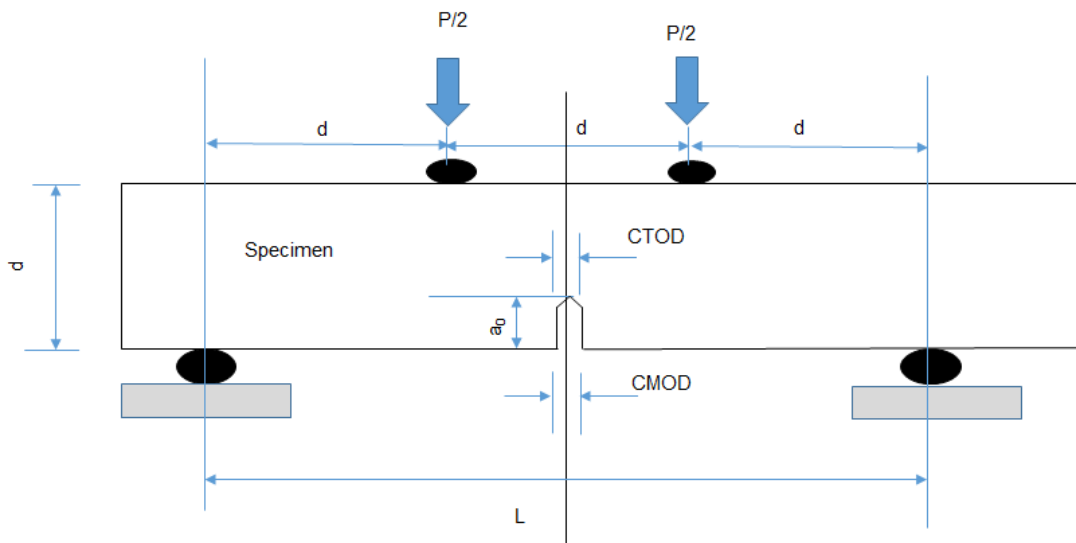
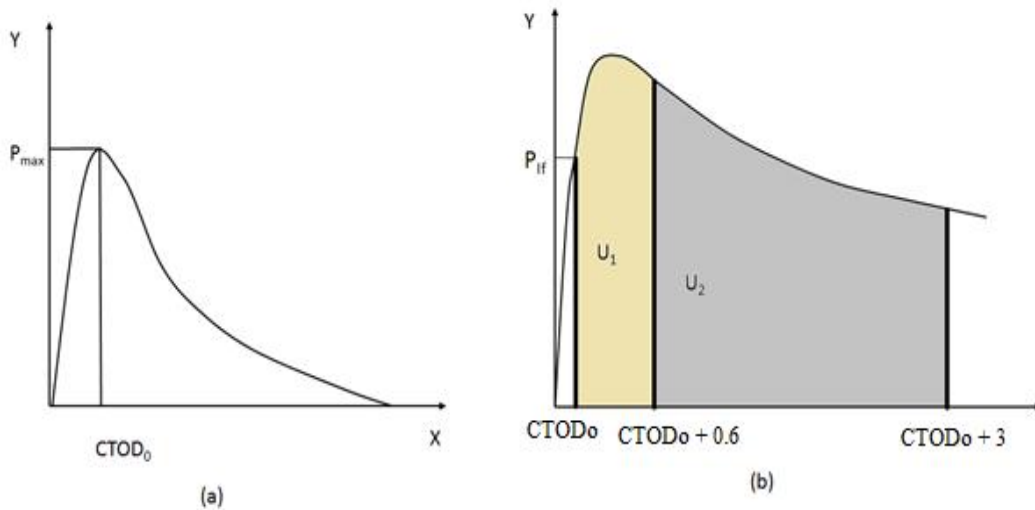


**Figure 2.12: Schematic diagram of the UNI 11309 four-point bending test setup**

The first-crack load which required subtracting the contribution due to matrix cracking is obtained by determining the value of CTOD corresponding to the peak load value obtained by performing four-point bending tests on plain concrete beams is determined ( $CTOD_0$ ) Figure 2.13 (a). In the absence of concrete specimens of the base is allowed the value of  $CTOD_0$  can be assumed equal to 25  $\mu\text{m}$ .



(a) Basic concrete load-CMOD diagram:  $CTOD_0$  meaning. (b) Load-CTOD diagram:  $U_1$  e  $U_2$  determination

**Figure 2.13: (a) Basic concrete load-CMOD diagram showing  $CMOD_0$ ; (b) Load-CTOD diagram:  $U_1$  e  $U_2$  determination**

The first-crack flexural strength is determined, according to UNI 11039, as follows:

$$f_{lf} = \frac{P_{lf}L}{b(h - a_0)^2}$$

where, L (mm) is the span between supports; b (mm) is the specimen width (equal to d); h (mm) is specimen depth (equal d); a<sub>0</sub> (mm) is the notch depth; and P<sub>lf</sub> (N) is the load value corresponding to CTOD<sub>0</sub> for the FRC specimen.

**The first and second Material's ductility** indexes, D<sub>0</sub> and D<sub>1</sub>, are defined by UNI 11039 by means of the equivalent flexural strengths  $f_{eq(0-0.6)}$  and  $f_{eq(0.6-3)}$  (MPa), which denote SFRC ductility in a defined range of crack mean opening displacement. Ductility indexes D<sub>0</sub> and D<sub>1</sub> are derived by means of the following equations:

$$D_0 = \frac{f_{eq(0-0.6)}}{f_{lf}} \qquad D_1 = \frac{f_{eq(0.6-3)}}{f_{eq(0-0.6)}}$$

where  $f_{eq(0-0.6)}$  is the equivalent strength (MPa) is calculated when the mean crack opening value is included between 0 and 0.6 mm,  $f_{eq(0.6-3)}$  is the equivalent strength (MPa) calculated when the mean crack opening value is included between (0.6 and 3) mm, derived from the following relationships:

$$f_{eq(0-0.6)} = \frac{l}{b(h - a_1)} \cdot \frac{U_1}{0.6}$$

$$f_{eq(0.6-3)} = \frac{l}{b(h - a_1)} \cdot \frac{U_2}{2.4}$$

Where U<sub>2</sub> and U<sub>3</sub> (10<sup>-3</sup> J) are the area under load - CTOD<sub>m</sub> curve for CTOD<sub>net</sub> intervals equal to 0-0.6 mm and 0.6-3 mm respectively Figure 2.13 (b). The areas are approximately proportional to the energy dissipated in the mean crack opening intervals considered.

#### 2.4.5 EN 14561

EN 14651 specifies a method of measuring a flexural tensile strength of metallic fibered concrete on moulded test specimen. Center point bend tests are performed on notched specimens with a nominal size (width and depth) of 150 mm, span length of 450mm and a length L so that 550 mm < L < 700 mm. Test is performed by increasing the *CMOD* at a

constant rate of 0,05 mm/min up to a CMOD value of 4mm. A schematic diagram of the EN 14651 test setup is shown in Figure 2.14.

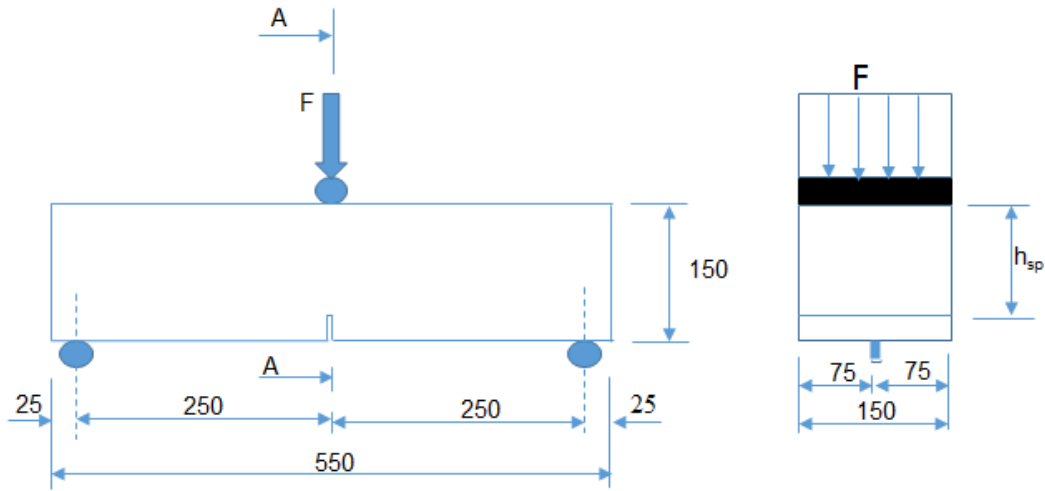


**Figure 2.14: Typical arrangement of measuring CMOD**

The methods provided for the determination of the limit of proportionality (LOP) and of a set residual flexural tensile strength values.

***Limit of proportionality***

$$f_{ct,fl} = \frac{3F_L L}{2bh_{sp}^2}$$

Where,  $f_{ct,fl}$  is the LOP (N/mm<sup>2</sup>);  $F_L$  is the load corresponding to LOP (N); L is span of specimen (mm); b is the width of specimen (mm);  $h_{sp}$  is the distance between the tip of notch and top of the specimen (mm).

***Residual flexural Tensile Strength***

$$f_{R,i} = \frac{3F_i L}{2bh_{sp}^2}$$

Where,  $f_{R,i}$  is Residual flexural Tensile Strength corresponding with CMOD = CMOD<sub>j</sub> or  $\delta = \delta$  (i= 1, 2, 3, 4) (N);  $F_i$  is the load corresponding to with CMOD = CMOD<sub>j</sub> or  $\delta = \delta_i$  (i = 1, 2, 3, 4) Figure 2.15.

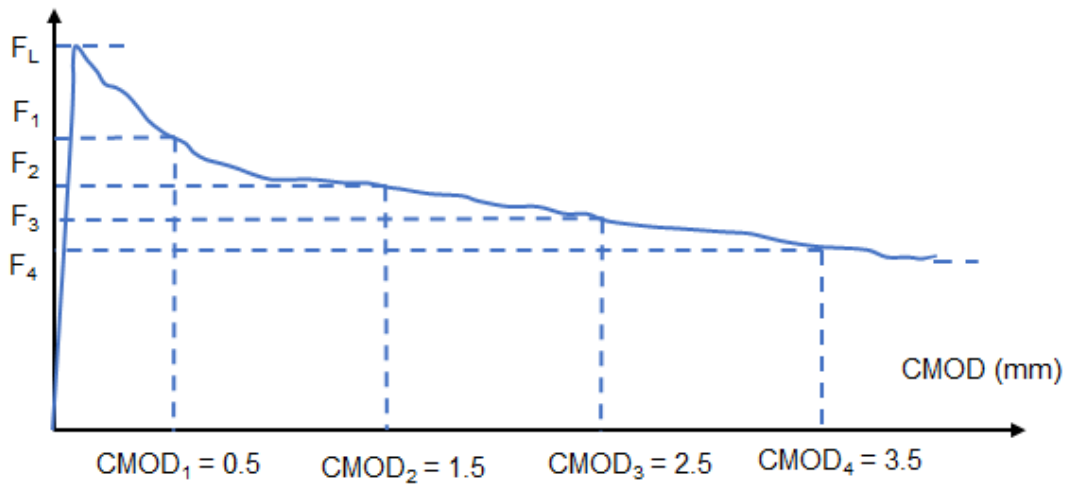


**Figure 2.15: Load-CMOD and  $F_j$  ( $j=1,2,3,4$ )**

Toughness index is used to measure the energy absorbed in deflecting a beam at specified amount, being the area under a load–deflection curve in three-point bending. A measure of toughness index from the results of the EN 14651 test has been proposed as the ratio of the area under the force-CMOD curve up to CMOD of 4 mm for the FRC specimen over that for the plain-concrete specimen [24].

Although the tests were conducted as per the ASTM C1018 procedure, the curves were analyzed using the post-crack strength (PCS) procedure.

For a beam with a width  $b$  and depth  $h$ , the post-crack strength  $PCS_m$  at a deflection of  $L/m$  is given by

$$PCS_m = \frac{E_{post,m}}{\frac{L}{m} - \delta_{peak}} \times \frac{L}{b \times h^2}$$

The terms used in the above equation are described in Figure 2.16. Note that  $PCS_m$  has units of stress and at a deflection equal to  $\delta_{peak}$ , the  $PCS_m$  value would coincide with the MOR of beam.

Fractions of the span,  $L/m$  (where ‘ $L$ ’ is the span of the beam, and ‘ $m$ ’ has different values ranging from 150 and 3000) area under the curve up to a deflection of  $L/m$  is termed “total energy” ( $E_{total,m}$ ). The pre-peak energy is subtracted from this total energy to obtain the post peak energy values,  $E_{post,m}$  corresponding to deflection  $L/m$  [25].

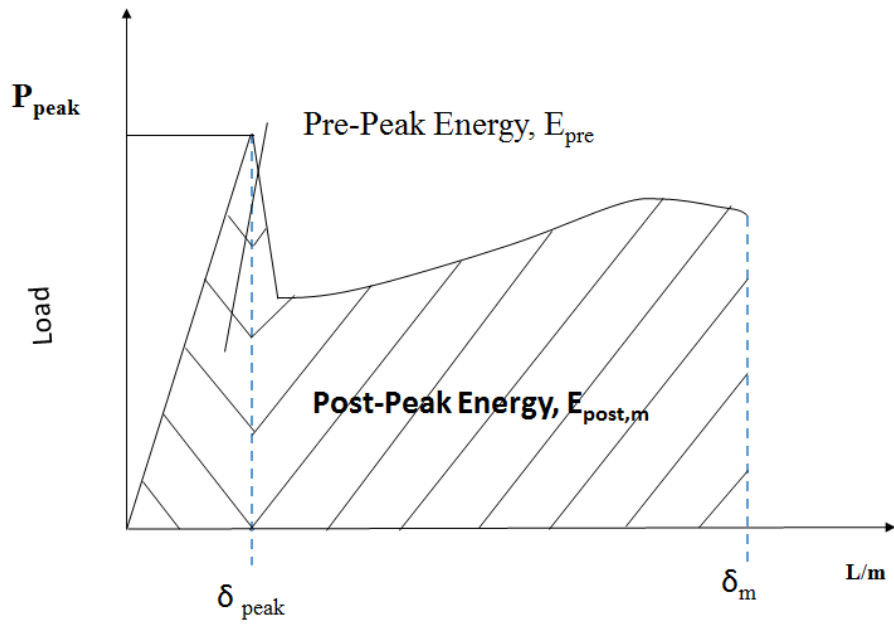


Figure 2.16: PCS analysis on a FRC beam



# Chapter 3

## Materials and Methods

This section presents the details of materials and experimental methods used in the study. The types of specimens, mix proportions and test methods employed are presented.

### 3.1 Cement

In the present investigation, commercially available 53 Grade ordinary Portland cement supplied by ACC Cement with Specific Gravity of 3.1 and Fineness modulus of 325 m<sup>2</sup>/kg was used for all concrete mixtures.

### 3.2 Fly Ash

Fly ash conforming to the requirements of IS 3812 and IS 1727 (1967) obtained from Manuguru heavy water unit was used as a supplementary cementitious material in concrete mixtures. The specific gravity and fineness modulus of the fly ash were 2.5 and 320 m<sup>2</sup>/kg, respectively.

### 3.3 Aggregates

Crushed sand with a specific gravity of 2.67 and fineness modulus of 2.83 was used as fine aggregate and crushed granite of specific gravity of 2.63 was used as coarse aggregate. Two different classes of coarse aggregate fractions were used: 10-4.75 mm and 20-10 mm.

### 3.4 Polypropylene fiber

FibreTuff™ Monofilament structural polypropylene fibers of 48mm and 60 mm length manufactured by Bajaj Reinforcements were used in this study. The fibers are made of a modified polyolefin and have a modulus of elasticity between 6 GPa to 10 GPa and tensile strength between 550 and 640MPa. The fibers are continually embossed surface anchorage mechanism to enhance bond. A photograph of the fibers used in this study is shown in Figure 3.1.



Figure 3.1: FibreTuff™ Monofilament structural polypropylene fiber

### 3.5 Admixture

Super plasticizer (Glenium) was used to increase the workability of freshly prepared fiber reinforced concrete.

### 3.6 Experimental program and Mix Proportions

Concrete mix design for the mix design procedure given in IS: 10262 was followed with minor modification for M35 grade. For a target mean strength of 43 MPa, two different water/cement ratios equal to 0.47 was considered (from Fig 2, curve E IS 10262-1982 for 53G). Taking into considerations, the minimum requirements for cement content in  $\text{kg/m}^3$  of concrete for M35 as per IS 456-2000 as  $300 \text{ kg/m}^3$ , cement content was fixed at  $340 \text{ kg/m}^3$ . Using this, the water content was determined. In the concrete mixture fine aggregate were taken as 45% of the total aggregate volume fraction. The weights of fine and coarse

aggregate were then calculated considering the specific gravities of coarse and fine aggregate.

The Concrete mixtures were produced at a constant water/Cement ratio of 0.47 and one control mixture and three different mixtures with different dosage of fiber were prepared. The control mixture contained no fiber. Concrete mixtures labelled PF3, PF4 and PF6 were produced with different dosage of fiber 3kg/m<sup>3</sup>, 4 kg/m<sup>3</sup> and 6 kg/m<sup>3</sup> by volume. The design mixtures are presented in Table 3 and the final batch weights of the different mixes for one cubic meter of concrete are presented in Table 3.1.

Table 3.1: Summary of weight proportion of the various mixes

Materials(kg/m <sup>3</sup> )	C1	PF3	PF4	PF6
Polypropylene fiber	-	3	4	6
OPC 53 grade cement	280	280	280	280
Fly ash(Manuguru)	60	60	60	60
Water/Cement Ratio	0.47	0.47	0.47	0.47
Admixture (%)	0.65	0.65	0.65	0.65
20 mm aggregates	520	520	520	520
10mm aggregates	520	520	520	520
Fine aggregates(river sand)	819	819	819	819
Water	165	165	165	165

### 3.6.1 Casting and Curing of Specimens

IS standard 150mm Cubes, 150mm X 300mm cylinder and 150 X 150 X 500 beams were cast from each mixture to evaluate compressive strength and toughness and ductility gain. Concrete was prepared using a drum mixer with a capacity of 0.25 m<sup>3</sup>. The ingredients were put into the mixer in the decreasing order of their sizes starting from 20mm aggregate to cement. Dry mixing of the aggregates and cement was done for two minutes and then water was added gradually in the rotating mixer and allowed to mix for 15 minutes. During the mixing process, the walls and bottom of mixer were scraped well to avoid sticking of mortar. After mixing, the slump was checked and noted down to ascertain the effects of differently proportioned blends on workability of concrete. Finally the fresh concrete was

placed in oiled moulds and compacted properly in three layers, each layer being tamped 35 times using a tamping rod. After the initial setting of concrete, the surface of the specimen was finished smooth using a trowel. Immediately after casting, all specimens were covered with plastic covers to minimize moisture loss. The specimens were stored at room temperature about 25°C. Specimens were demoulded 24 hours after casting and kept in curing water tank.

### **3.7 Test Methods**

An experimental program is designed to study the influence of fiber on the flexural load response, toughness and ductility of concrete. The test program consists of evaluating each mixture for slump, compressive strength, load response and post-peak load carrying ability from flexural response in three and third-point bending on notched and unnotched specimens, respectively.

#### **3.7.1 Slump**

Slump was used to find the workability of fresh concrete where the nominal maximum size of aggregate does not exceed 38 mm. slump cone was used to find the slump of the concrete as per the requirements of IS 1199-1959.

#### **Procedure**

Oil is applied on the base plate and interior surface of the slump cone. The slump cone is kept on a levelled surface and filled with fresh concrete in three layers, approximately one-third of height of the cone. Each layer is tamped 25 times with a tamping rod. After compacting the top layer, the concrete surface is struck off. The slump cone is removed by raising it slowly in a vertical direction. The slump is recorded as the height to which concrete settles from the height at the highest point of the concrete.

#### **3.7.2 Compression Strength Testing**

A 2000kN digital compressive testing machine is used for determine the compressive strength of hardened concrete as per the requirements of IS 516-1959 using standard 150mm cubes.

## **Procedure**

For cubes, before starting the test the weight of the sample are recorded. The plates of the machine are cleaned and the specimen is kept centrally between the two plates. Load is applied gradually on the specimen at a load rate of 5.15kN/s up to failure. Once the sample is failed, the failure pattern is recorded and the compressive strength is calculated from the maximum load recorded in the test.

### **3.7.3 Flexural Test**

Flexural testing machine with servo hydraulic closed-loop test machine is used to determine the toughness and ductility as per ASTM C1609-10 and EN 14651.

#### **a) Four-point-bending test (For Un-notch beam)**

This test method utilizes 150 x 150 x 500 mm beams tested on a 450 mm span. The testing is done using a servo-controlled test machine where the net deflection of the centre of the beam is measured and used to control the rate of increase of deflection. Testing is done as per ASTM C1609 to capture the portion of the load-deflection curve immediately after the first-peak. The loading and specimen support system applies third-point loading to the specimen without any eccentricity or torque. A photograph of the test setup is shown in Figure 3.2. The fixtures used in the testing allow free rotation on their axes. Linear variable displacement transducers (LVDT) are used to ensure accurate determination of the net deflection at the mid-span. Rectangular jig is clamped to the specimen at mid-depth directly over the supports. Two displacement transducers are mounted on the jig at mid-span, one on each side, to measure deflection through contact with appropriate brackets attached to the specimen. The average of the measurements represents the net deflection of the specimen exclusive of the effects of seating or twisting of the specimen on its supports. The loading is applied such that the net deflection of the specimen increased at a constant rate of 0.04 mm/min up to a net deflection of  $L/900$ . Thereafter, beyond  $L/900$  and up to a deflection of  $L/150$ , loading rate is kept constant at 0.08 mm/min. Beyond  $L/150$  and up to the end point deflection, the rate of loading is kept constant at 0.158mm/min. The testing is continued till the specimen fails.



**Figure 3.2: Test setup as per ASTM C 1609**

**b) Three-point-bending test (For notch beam)**

The test procedure adopted was consistent with the guidelines given by EN 14651:2005 and 150 X 150 X 500 (height X width X length) mm<sup>3</sup> prismatic specimens were tested in the three-point bending configuration as shown in Figure 2.14. A notch of 25mm depth was introduced at the mid-span using a circular saw as per the guidelines given in EN 14651:2005. The flexure test was conducted in crack mouth opening displacement control by increasing the CMOD at a prescribed rate. The corresponding deflection of the beam was measured using the rectangular jig clamped to the specimen at mid-depth directly over the supports. The testing machine had sufficient stiffness to avoid unstable unloading phenomena in the softening branch of the load-CMOD curve. A photograph of the test setup is shown in Figure 3.3



**Figure 3.3: Test setup as per EN 14651-2005**

The notched beam was tested with a span equal to 450 mm during the tests, the rate of increase of the CMOD was controlled in two stages, at 0.05 mm/min for CMOD less than 0.1 mm and at 0.2 mm/min for CMOD greater than 0.1 mm. All the tests were ended at

when the CMOD reached a value of 4 mm. Figure 2.15 shows a generic force-CMOD curve obtained from the beam tests.

### **3.7.4 Digital Image Correlation -DIC (For notch beam)**

2-D, full-field optical technique known as digital image correlation (DIC) was performed to study the full-field displacement field due to crack propagation in the concrete specimens. DIC is a data analysis procedure that uses the mathematical correlation method to analyze digital images of a specimen undergoing deformation. This technique offers the advantage of obtaining spatially continuous measurements of displacements. The correlation between the undeformed reference image and the deformed image was used to obtain a two-dimensional displacement field for all points on the specimen surface. The displacement fields were computed through a correlation of grey levels between the reference image and the images of the specimen undergoing deformation using the commercially available software, Vic 2D™. The strain fields were then computed from the gradients of the displacement field.

For using DIC a sprayed on speckle pattern was created on the specimen surface prior to beginning the load test. In order to create a characteristic pattern on the specimen surface, the specimen was sprayed by a white paint to obtain a white background. Black speckles were then deposited on the white surface by randomly spraying the black paint on the background. The testing specimen then was installed into a loading frame and digital images of the specimen with speckle pattern were acquired at various load points using a 5 mega pixel camera and stored in a computer for post-processing. A photograph of the test setup showing the DIC test setup is shown in Figure 3.4.



**Figure 3.4: Test setup of DIC**

# Chapter 4

## Result and Discussion

### 4.1 Introduction

Improvements in mechanical properties on using fibers are a result of crack closing stresses provided by fibers which have a direct influence on the ductility, load carrying capacity and toughness. The improvements depend upon the crack closing stresses generated by the fibers. The efficiency of fibers depend the ability of fibers to contribute during localization and propagation of a crack. For a given fiber type, fiber volume fraction is a primary variable which controls the properties of the composite.

The results of an investigation into the influence of the macro synthetic fibers on the fresh and hardened properties of concrete are presented in this chapter. These include results of workability tests of fresh concrete, results of compression tests of cube and cylinder at 90 days respectively, and results of beam flexural tests at 90 days. The results of the flexural response are interpreted in terms of the influence of fibers on crack propagation in fiber reinforced concrete.

### 4.2 Workability of fresh SPFRC

Slump of concrete measured immediately after mixing for the control mixture and the structural polypropylene fibre reinforced concrete (SPFRC) mixtures is tabulated in Table 4.1 and shown plotted as a function of fiber content in Figure 4.1. In all mixtures a PCE based superplasticizer was used and no adjustment to water content was done for fiber addition considering the hydrophilic nature of polypropylene. The superplasticizer dosage was kept constant in all mixtures. The results indicate that slump (or the workability) decreases with increase in fibre content. Slight bleeding was observed in the control



mixture. The aggregate for the 3kg/m<sup>3</sup> mix of 48 mm length were in a wet state. The added water in the mix was adjusted based on an estimated excess water content in the aggregate. However during casting bleeding was observed in the mix. Aggregate for all other mixes were taken in an air dry state and extra water required for saturated surface dry state was added to the mix. No bleeding was observed in any other mix.

Increasing fiber content also decreased the bleeding and increased the cohesiveness of the mix. The decrease in the workability in SPFRC for both mm and 60mm fiber lengths is in conformity with previous observations from fibrillated polypropylene fibers [7]. The fibers bind the matrix giving it uniformity reducing segregation and bleeding.

Table 4.1: Properties of the fresh concrete measured during the casting of the different sets of specimens.

	Fiber length (l <sub>f</sub> )	Slump (mm)
Control	48	220
3kg/m <sup>3</sup>		190
4kg/m <sup>3</sup>		130
6kg/m <sup>3</sup>		110
Control	60	175
3kg/m <sup>3</sup>		155
4kg/m <sup>3</sup>		135
6kg/m <sup>3</sup>		110

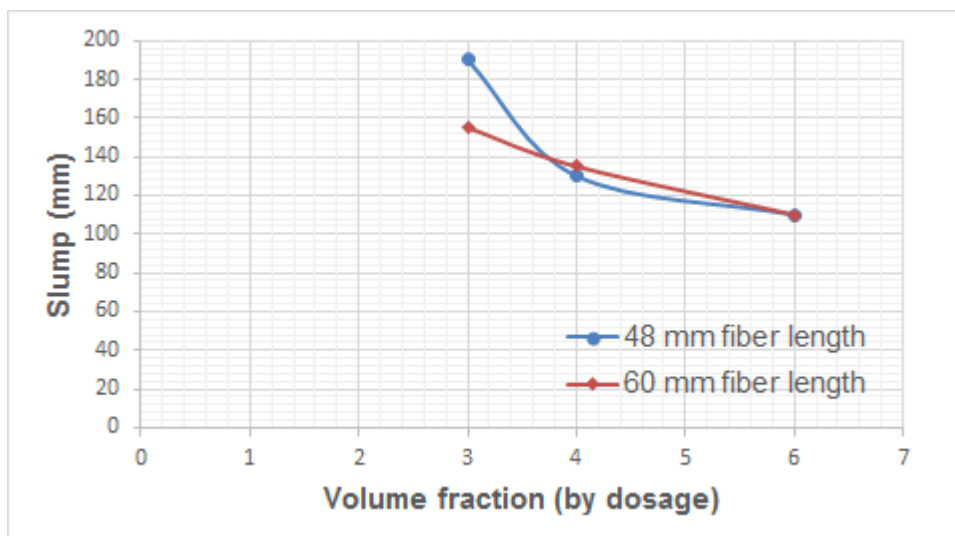


Figure 4.1: Effect of volume fraction on slump

### **4.3 Compressive strength**

The 90 day compressive strength from standard 150mm cubes for control and SPFRC with 48mm fibers obtained are tabulated in Table 4.2. It is immediately obvious that the variability within each mix is low, the variation of compressive strength with fiber content does not show a clear trend. While the compressive strengths from control and SPFRC with 4 and 6 kg/m<sup>3</sup> are comparable within the range of experimental scatter evident in the variability within the batch, the compressive strengths from 3 kg/m<sup>3</sup> are significantly lower. This may be explained considering the excess water in this mix due to the wet aggregate. Since in all other mixes aggregate were taken in air dry state, the excess water was likely under-estimated leading to excess water in the mix.

The results indicate that the addition of macro synthetic polypropylene fibers at quantities up to 6 kg/m<sup>3</sup> has no effect on the compressive strength. The minor differences noticed are expected variation in sample preparation, and to variations in the actual air contents of the hardened concrete and the differences in their unit weights. These results are in agreement with the observation from fibrillated polypropylene fibers [7].

The addition of polypropylene fibers had a significant effect on the mode and mechanism of failure of concrete cylinders in compression test. The fiber reinforced concrete failed in a more ductile mode, whereas plain control concrete cylinders typically shatter due to an inability to absorb the energy release imposed by the test machine at failure.

Table 4.2: Compressive strength for cube

	Compressive strength (MPa)	Average compressive strength (MPa)	Standard deviation (MPa)
Control -1	61.2	64.76	3.28
Control -2	67.5		
Control -3	61.2		
Control -4	67.5		
Control -5	66.4		
3kg/m <sup>3</sup> -1	59.4	58.34	3.40
3kg/m <sup>3</sup> -2	61.1		
3kg/m <sup>3</sup> -3	60.2		
3kg/m <sup>3</sup> -4	52.5		
3kg/m <sup>3</sup> -5	58.5		
4kg/m <sup>3</sup> -1	69.4	70.20	0.54
4kg/m <sup>3</sup> -2	69.9		
4kg/m <sup>3</sup> -3	70.6		
4kg/m <sup>3</sup> -4	70.4		
4kg/m <sup>3</sup> -5	70.7		
6kg/m <sup>3</sup> -1	64	65.66	1.78
6kg/m <sup>3</sup> -2	66.6		
6kg/m <sup>3</sup> -3	63.7		
6kg/m <sup>3</sup> -4	66.1		
6kg/m <sup>3</sup> -5	67.9		

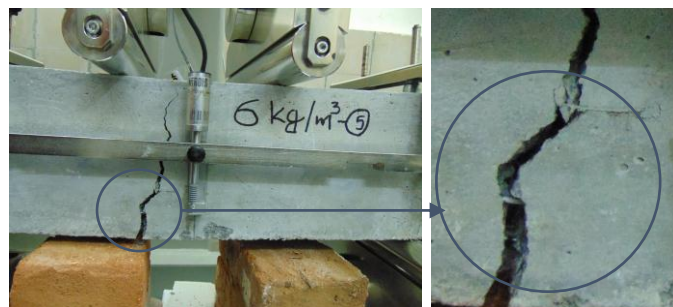
#### 4.4 Flexural test results as per ASTM C 1609 (For unnotch beam)

The load-deflection responses of the control and SPFRC beams in flexure are shown in Figure 4.3 a through d. The failure in both control and SPFRC beams were due to the formation of a single crack in the constant moment region of the beam. All beams, both control and SPFRC exhibit nonlinearity in the load response immediately following the initial linear response, before peak load. Following the peak load, which is associated with the localization of a single crack, while the control beams failed suddenly in a brittle manner the SPFRC specimens exhibit significant post-peak response indicating load carrying ability even after the formation of a crack. The brittle failure in a control specimen which resulted in splitting the specimen in two pieces is shown in Figure 4.2 (a). Some of the control specimens indicate a load drop immediately after the peak. However, the load response in the post peak could not be obtained in a controlled manner. A photograph of the specimen with 6kg/m<sup>3</sup> fibers taken at a deflection of 4 mm with a visible crack in the constant moment

region is shown in Figure 4.2 (b). The fibers crossing the crack are shown in the inset of the figure. Therefore, the fibers are responsible for preventing the brittle failure and providing load carrying capacity. There is clearly an increase in the post-peak load carrying capacity with the addition of fibers. In SPFRC, there is a drop in load immediately after peak, following which the beams with 3 and 4 kg/m<sup>3</sup> showed an essentially constant load carrying capacity with increasing deflection with an indication initial hardening followed by softening with increasing deflection. Even in specimens with 3 and 4 kg/m<sup>3</sup> fibers, the load drop could not be obtained in a stable manner for all specimens. The lack of control was due to inability of the control algorithm to compensate for sudden load drops associated with abrupt crack advance. The beams with 6 kg/m<sup>3</sup> show a prominent hardening response following the initial drop after peak load. All SPFRC beams indicate residual load carrying capacity up to a deflection 3 mm. While the 3 kg/m<sup>3</sup> beams indicate a decrease in load carrying capacity beyond 1.5 mm deflection, the 4 and 6 kg/m<sup>3</sup> beams show a decrease in load carrying capacity after a deflection of 3 mm



(a)



(b)

**Figure 4.2: Failure of beam**

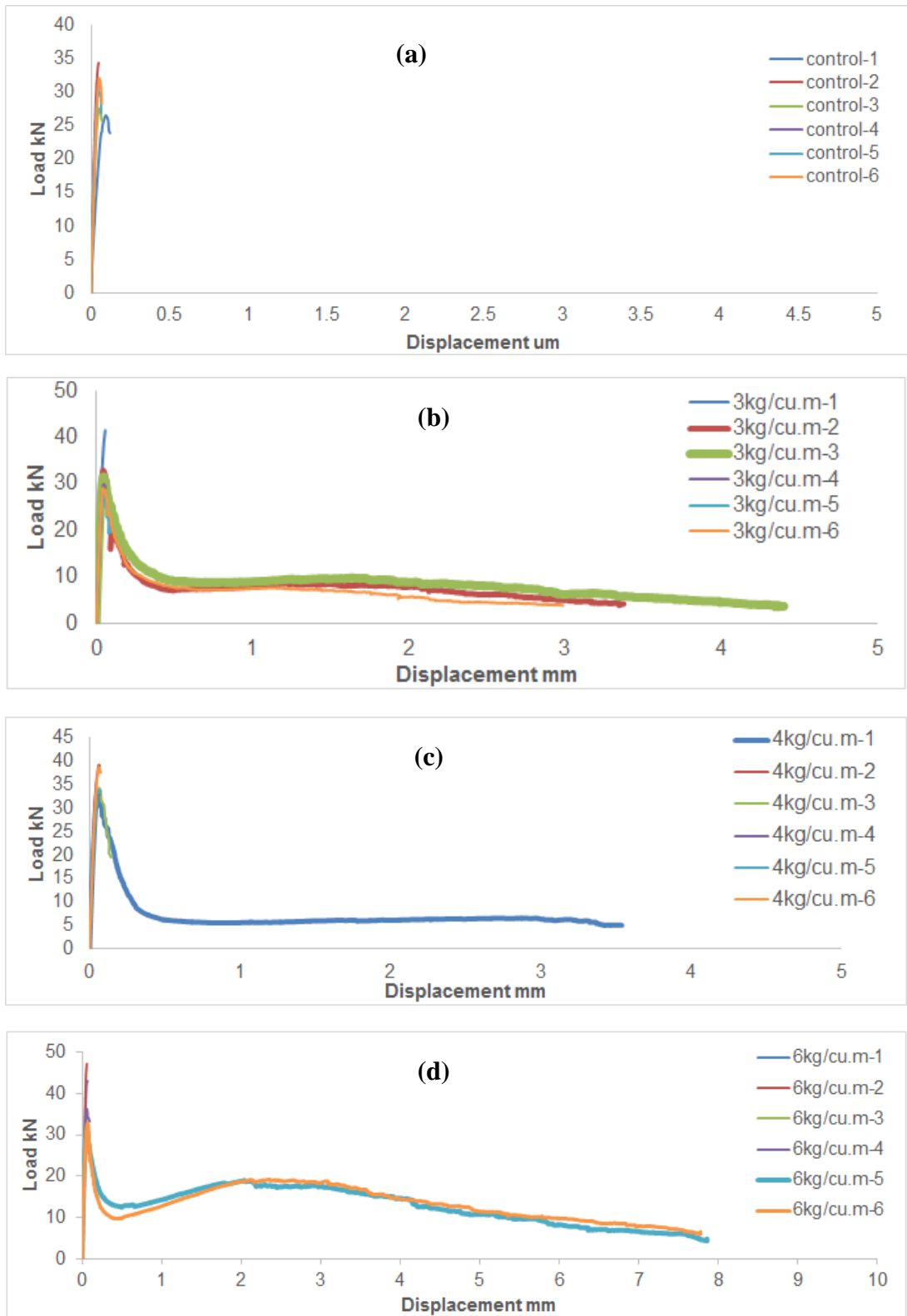
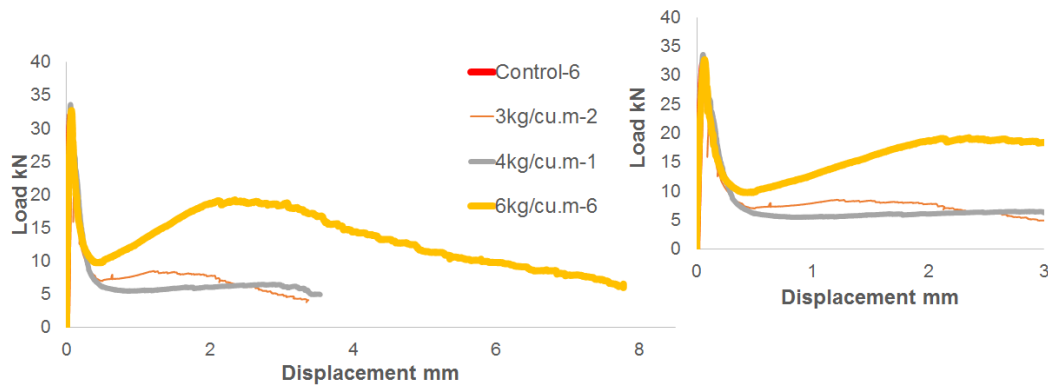


Figure 4.3: Load vs Displacement curve for control, 3kg/m<sup>3</sup>, 4kg/m<sup>3</sup> and 6kg/m<sup>3</sup>

SPFRC beams exhibit post-peak residual strength and toughness, which is attributed to crack bridging provided by fibers. A comparison of load responses from typical SPFRC specimens reinforced with 3, 4 and 6 kg/m<sup>3</sup> fibers is shown in Figure 4.4. The load response up to a deflection of 3 mm is shown in the inset of the Figure 4.4. It is seen that the peak load is not affected by the presence of fibers is shown in Figure 4.5 and even the pre peak behaviour is similar for the control and the SPFRC specimens at the three fiber dosages. The pre-peak peak non-linearity, which is associated with the initiation of crack formation indicates that fibers do not play role before localization of crack. After peak load, in case of control specimens, there is no mechanism to arrest the crack and the load drop could not be obtained in a controlled manner. In SPFRC, after peak load there is progressive decrease in the load with a small corresponding increase in deflection. This part of the response (shown better in the inset) indicates the response for the three fiber dosages is nominally similar, which suggests that this part of the response is not significantly influenced by fiber content. Thus, the load decrease in the post-peak response immediately after the peak is dominated by crack propagation in the matrix. The load which can be safely supported decreases with an increase in the crack length. The propagation of the crack in the matrix results in an increase in the compliance of the beam, which produces a rapid increase in deflection accompanied by a decrease in the load. After the load decrease there is a local minimum following which the load starts to increase with increasing deflection. In 3 and 4 kg/m<sup>3</sup>, the increase is marginal, there is considerable recovery in the load carrying capacity in 6 kg/m<sup>3</sup>. The increase in load carrying capacity with deflection suggests a change in the rate of crack propagation and the crack bridging forces. The number of fiber scattered over the depth at the location of crack provide additional crack bridging forces. In case of 6kg/m<sup>3</sup> SPFC, because the number of fibers that come into play to arrest crack are significantly larger than the 4kg/m<sup>3</sup>, the post peak decrease is stopped earlier. The local minimum in the post-peak load response occurs at a higher load for higher fiber content. Further, on increasing the deflection, the increase in resistance of the beam suggests an increase in the tensile capacity provided by the fibers crossing the crack. The effective tensile resistance from fibers across the crack also exhibits a hardening response. The resistance to crack opening comes from either pull out of the fiber from the matrix or fiber extension which could ultimately lead to fiber fracture. The increase in the total tensile resistance after the local minimum can be attributed to the increased resistance provided by additional fibers across the crack face with an increase in crack length and the additional stress due to increased resistance to pullout of individual fibers.

The load response in flexure can now be delineated in terms of three distinct stages, each associated with a different mechanism of resistance. The first stage consists of the pre-peak load response, where fibers play an insignificant role. Following localization, the initial part of post peak associated with crack propagation in the cementitious matrix is the second stage. The role of fibers becomes significant in determining the end of the second stage, where the local minimum is achieved. The local minimum in the load can be identified as the crack arrest load (CAL). Following CAL, the hardening response associated with the fiber pullout response is the third stage in the flexural response of SPFRC.



**Figure 4.4: Comparison typical specimen of Load vs Displacement curve for control and 3, 4 and 6kg/m<sup>3</sup>**

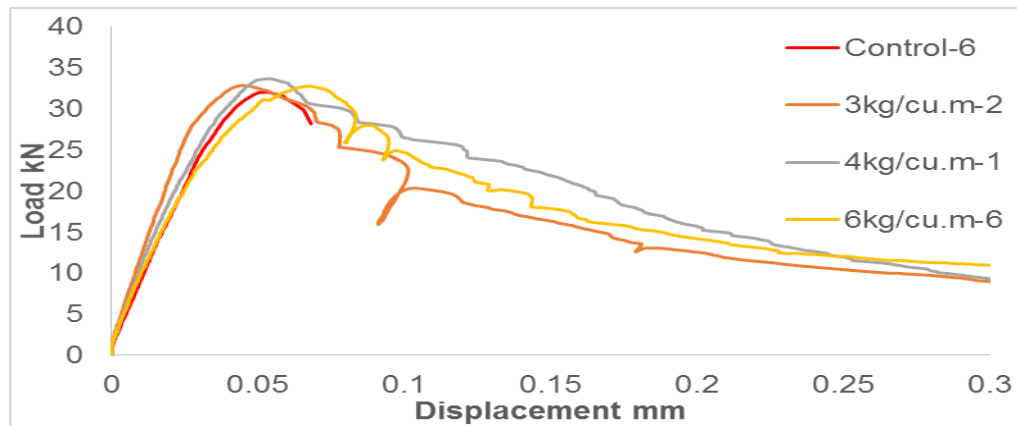


**Figure 4.5: Comparison typical specimen of Peak Load for PC and 3, 4 and 6kg/m<sup>3</sup>**

The the residual strengths  $f_{600}^D$ ,  $f_{150}^D$  obtained at deflections corresponding to span/600 and span/150 obtained from ASTM 1609 are shown in Table 4.3. As is evident from Table 4.3, the residual strengths  $f_{600}^D$ ,  $f_{150}^D$  is clearly increase with fiber content and the toughness parameters  $T_{150}^D$  show double energy required to break the specimen for 6 kg/m<sup>3</sup> compare to 3 kg/m<sup>3</sup> Table 4.5 .

Table 4.3: Test results for all specimens tested as per ASTM C-1609

Specimen No.	P (kN)	F (MPa)	P <sub>600</sub> <sup>D</sup> (kN)	P <sub>150</sub> <sup>D</sup> (kN)	f <sub>600</sub> <sup>D</sup> (MPa)	f <sub>150</sub> <sup>D</sup> (MPa)	T <sub>150</sub> <sup>D</sup>	R <sub>T,150</sub> <sup>D</sup> (%)
3kg/m <sup>3</sup> -2	32.823	4.376	7.47	4.98	0.996	0.663	20169.996	20.484
3kg/m <sup>3</sup> -3	31.493	4.199	8.76	6.15	1.168	0.82	25277.058	26.754
3kg/m <sup>3</sup> -6	29028	3.87	7.20	3.85	0.96	0.513	17387.205	19.966
4kg/m <sup>3</sup> -1	33.641	4.485	5.63	6.33	0.75	0.844	17816.244	17.653
6kg/m <sup>3</sup> -5	29992	3.999	1.31	17.50	1.745	2.334	40067.08	44.531
6kg/m <sup>3</sup> -6	32753	4.367	3.2	18.44	4.266	2.458	39744.903	40.449

Table 4.4: flexural toughness indices using ASTM C-1018

Specimen No.	I <sub>5</sub>	I <sub>10</sub>	I <sub>20</sub>	R <sub>5,10</sub>	R <sub>10,20</sub>
3kg/m <sup>3</sup> -2	3.51	5.155	6.825	32.9	16.7
3kg/m <sup>3</sup> -3	3.352	5.167	7.45	36.3	22.83
3kg/m <sup>3</sup> -6	3.548	5.429	7.432	37.62	20.03
4kg/m <sup>3</sup> -1	3.379	4.927	6.137	30.96	12.1
6kg/m <sup>3</sup> -5	3.31	5.045	7.313	34.7	22.68
6kg/m <sup>3</sup> -6	2.858	3.949	5.778	21.82	18.29

Table 4.5: flexural toughness indices using JSCE SF 24

Specimen No.	T <sub>JSCE</sub>	F <sub>JSCE</sub>
3kg/m <sup>3</sup> -2	20169.996	0.896
3kg/m <sup>3</sup> -3	25277.058	1.123
3kg/m <sup>3</sup> -6	17387.205	0.77
4kg/m <sup>3</sup> -1	17816.244	0.792
6kg/m <sup>3</sup> -5	40067.08	1.781
6kg/m <sup>3</sup> -6	39744.903	1.766



#### **4.5 Flexural test results as per EN 14651-2005 (For notch beam)**

The load-CMOD responses for the control and the SPFRC specimens are shown in Figure 4.6 a through d. The behaviour from the notched beams is nominally similar to the observed response from unnotched beams. The control specimens exhibit a steady decrease in the post-peak load carrying capacity with an increase in CMOD following a non-linear pre-peak response up to peak load. Use of CMOD control allowed for obtaining the entire post peak response in a controlled manner. The post-peak softening response is associated with unstable crack growth following localization. The initiation and propagation of crack from the notch in SPFRC leads to a 3-stage response observed earlier in the case of unnotched specimens. A comparison of load CMOD curve of typical control and SPFRC with fiber contents equal to  $3\text{kg/m}^3$ ,  $4\text{kg/m}^3$  and  $6\text{kg/m}^3$  are shown in Figure 4.7. The variations in the peak load are found to be within the range of experimental scatter for each suggesting that the fibers do not influence the peak load. Further, immediate post-peak softening response after peak load is also identical for control and SPFRC. After peak load, the decrease in the load with increasing CMOD is produced by the increasing compliance associated with cracking in the matrix. The initial drop in the load in the post-peak softening is not influenced by the presence of fibers. The influence of larger number of fibers across the crack results in a significant deviation from the load response with increasing CMOD for the  $6\text{ kg/m}^3$  fiber content when compared with the control and the SPFRC with 3 and 4  $\text{kg/m}^3$  fibers. At any CMOD, the SPFRC with  $6\text{ kg/m}^3$  supports a higher load when compared with SPFRC with 3 and 4  $\text{kg/m}^3$  fibers. The CMOD response indicates the contribution of fibers in the post-peak softening more sensitively than evident in the load deflection response of un-notched specimens. The distinctive crack arrest loads for 3, 4 and  $6\text{ kg/m}^3$  and the hardening responses associated with increased resistance provided by pullout of fibers is clearly identified in the responses.

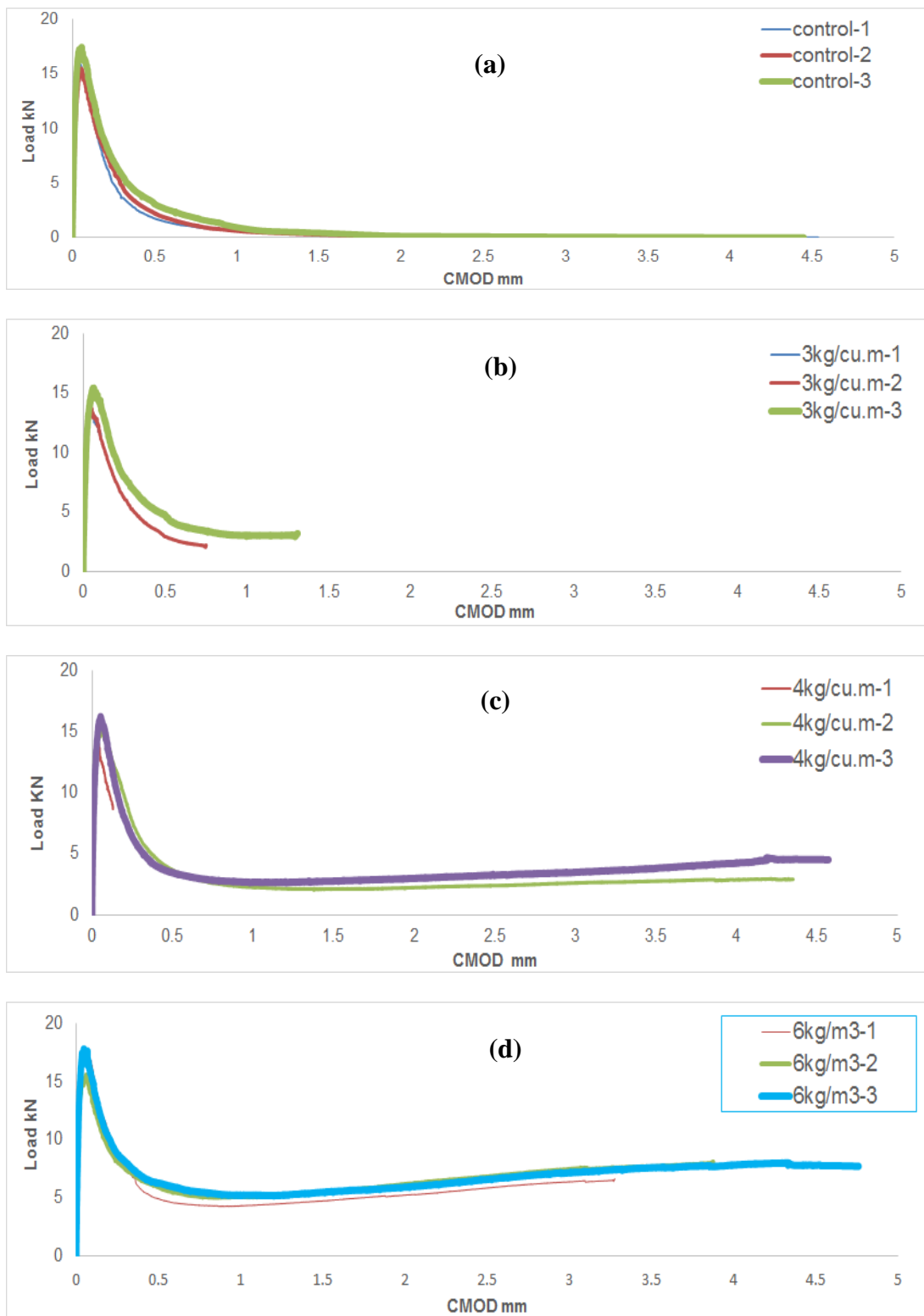
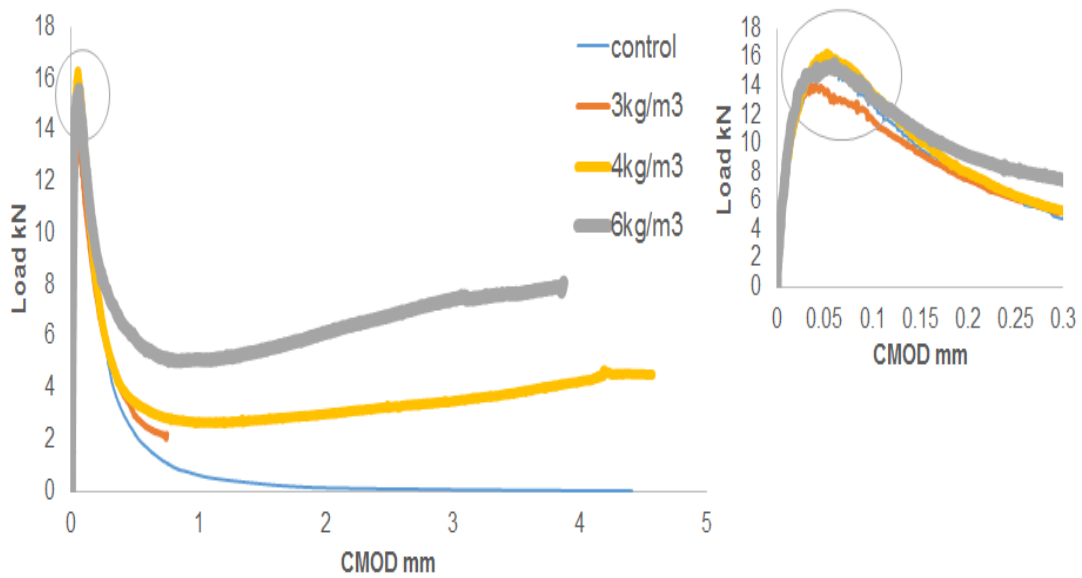


Figure 4.6: Load vs CMOD curve for control, 3kg/m<sup>3</sup>, 4kg/m<sup>3</sup> and 6kg/m<sup>3</sup>



**Figure 4.7: Comparison of typical specimen of Load vs CMOD curve for PC and 3, 4 an 6kg/m<sup>3</sup>**

As is evident from Table 4.6, the residual load and residual strengths is clearly increase with fiber content. In case of 6kg/m<sup>3</sup>, residual load is increase half of the load at limit of proportionality.

Table 4.6: Stress at LOP and Residual Strength and using EN 14651-2005

Specimen No.	$F_L$ (kN)	$f_{ct,L}^f$ (MPa)	$F_1$ (kN)	$F_2$ (kN)	$F_3$ (kN)	$F_4$ (kN)	$f_{R,1}$ (MPa)	$f_{R,2}$ (MPa)	$f_{R,3}$ (MPa)	$f_{R,4}$ (MPa)
3kg/m <sup>3</sup> -1	13.27	3.82	0	0	0	0	0	0	0	0
3kg/m <sup>3</sup> -2	14.09	4.06	2.93	0	0	0	0.84	0	0	0
3kg/m <sup>3</sup> -3	14.96	4.31	4.75				1.37			
4kg/m <sup>3</sup> -1	12.94	3.73	0	0	0	0	0.00	0	0	0
4kg/m <sup>3</sup> -2	15.09	4.34	3.67	2.12	2.40	2.77	1.06	0.61	0.69	0.80
4kg/m <sup>3</sup> -3	16.02	4.61	3.45	2.77	3.23	3.81	0.99	0.80	0.93	1.10
6kg/m <sup>3</sup> -1	16.99	4.89	4.90	4.74	5.85	0	1.41	1.36	1.68	0.00
6kg/m <sup>3</sup> -2	15.34	4.42	5.94	5.45	6.8	7.68	1.71	1.57	1.96	2.21
6kg/m <sup>3</sup> -3	17.73	5.11	6.25	5.47	6.59	7.59	1.80	1.57	1.90	2.19

#### 4.6 Fiber distribution

To check the distribution of the Structural polypropylene fibers on the specimen's fracture surface a grid, 25 mm x 25 mm was drawn on the fractured surface as shown in Figure 4.8 and the fibers that were visible in each cell were counted. The results of the fiber counts in at different location of the fractured surface of the unnotched and notched specimens tested

as per ASTM 1609 and EN 14651-2005 respectively are shown in Appendix I. Additionally, the load response and the residual strengths for the respective specimen are also shown in the appendix for comparison. A strong correlation between the total fiber count and the load response of the unnotched specimens is observed; specimens with larger fiber counts gave controlled post-peak softening response, while the specimens with lower fiber exhibited uncontrolled failure in the post-peak. There is also a correlation between fiber distribution across the depth and the residual strength at increasing deflection.

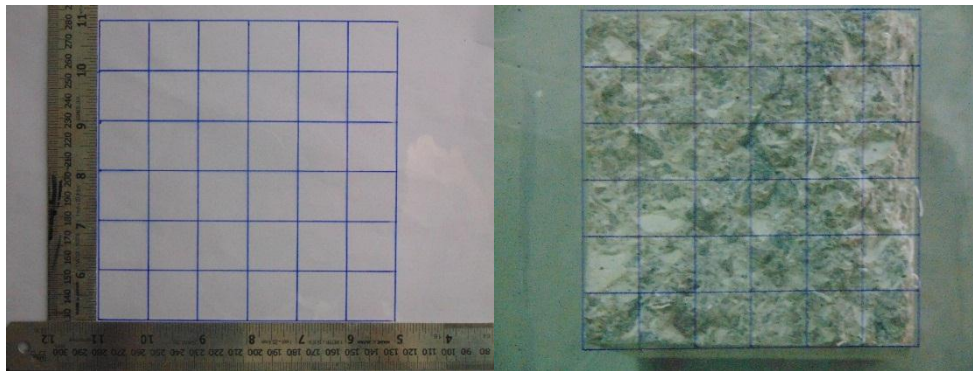


**Figure 4.8: Grid of 1 inch X 1 inch for fiber distribution**

#### **4.7 DIC test result**

Typical result showing strain at x direction ( $\epsilon_{xx}$ ) at distinct point on the load response of a notched specimen with  $6\text{kg/m}^3$  tested CMOD control is shown in Figure 4.9. It can be observed that strain localization is initiated close to the peak load and leads to the formation of single crack emanating from the notch in the post peak. The growth of the crack can clearly be identified with softening in the post peak load response.

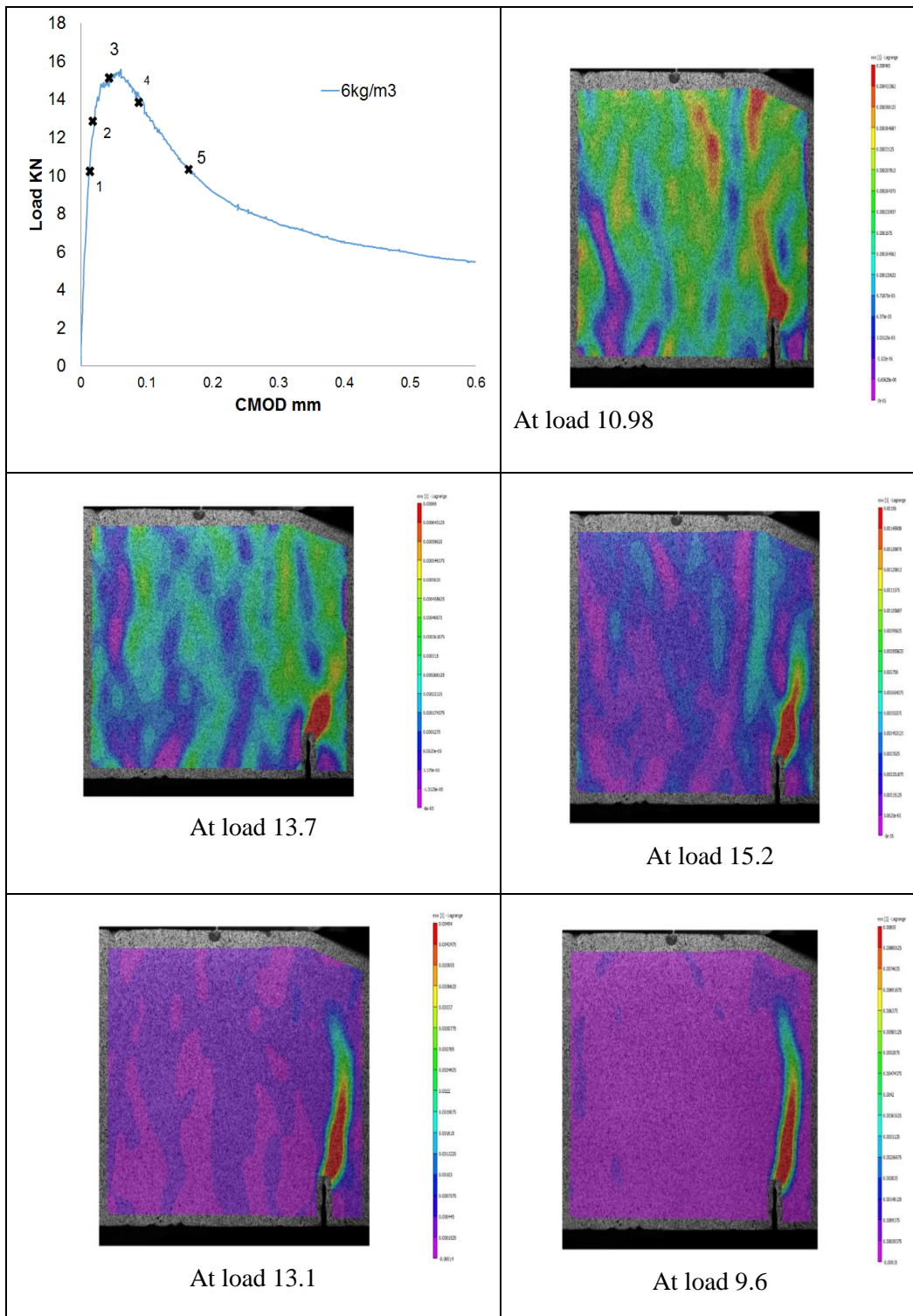


**Figure 4.9: Load response of a specimen with 6kg/m<sup>3</sup> and  $\epsilon_{xx}$  at distinct points in the load response on the load response.**

$\epsilon_{xx}$  along the distinct lines located at different heights above the notch were obtained. The location of the line are given in Table 4.7 and shown in Figure 4.10. The variation in  $\epsilon_{xx}$  along line 1, located just above the notch at distinct point in the load response for control,  $4\text{kg/m}^3$  and  $6\text{kg/m}^3$  are shown in Figure 4.11. The strain localization is evident in the very large increase in strain at the location of the notch. The increase in strain within a band close to the notch is indicative of strain localization. The strain localization is noticed over a finite width, along the strip. The width associated with localization appears to remain constant during the post peak load response. This indicates that strains in a finite region close to the crack plane are influenced by the crack. This region has also been called the hinge length [26]. The available data indicate that the hinge length remains constant during as the crack propagates in the matrix. From the available data, an estimate of the hinge length was obtained as the length over the strip, where the strains deviate by more than two times the standard deviation of the strain in the region away from the notch. The hinge length determined from the image analysis are tabulated in Table 4.8. It can be seen that hinge lengths slightly with the addition fibers.

Table 4.7: Location of lines

	<b>Distance from bottom of beam</b>
First line	31
Second line	44
Third line	70
Fourth line	99
Fifth line	118

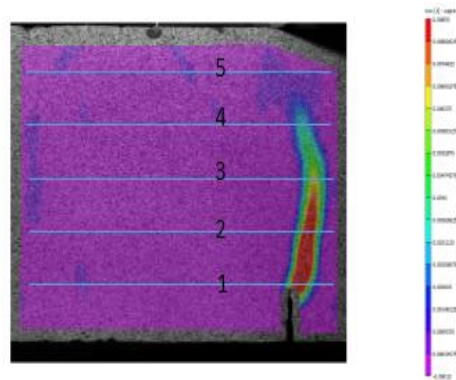


Figure 4.10: Location of lines

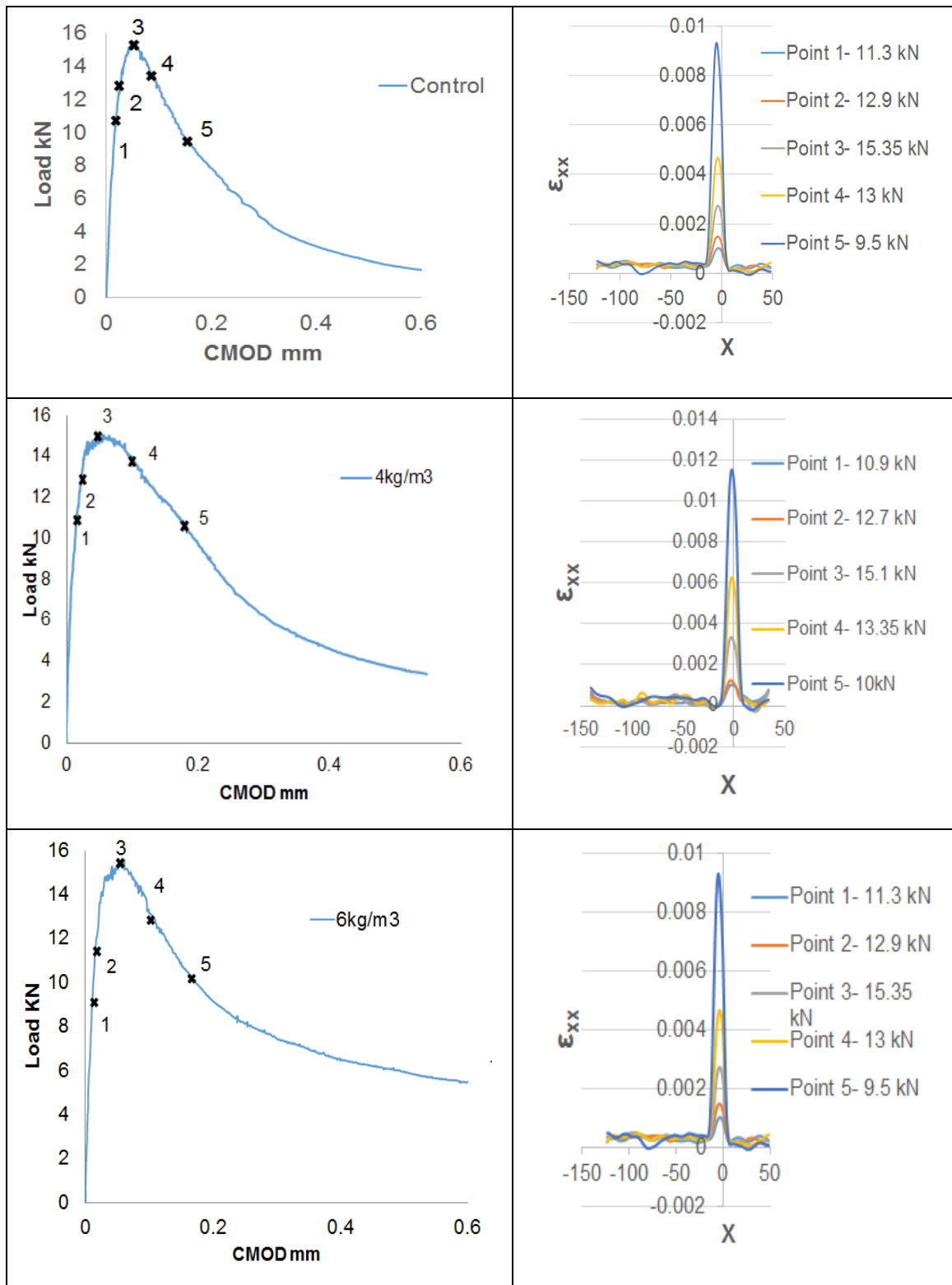


Figure 4.11:  $\epsilon_{xx}$  along line one for control, 4kg/m<sup>3</sup> and 6kg/m<sup>3</sup>

Table 4.8: Hinge length

Hinge length (mm)	Control	4kg/m <sup>3</sup>	6kg/m <sup>3</sup>
At first line	21.09	20.35	29.09
At second line	29.15	24.26	23.2
at Third line	27.23	25.83	22.8
At Fourth line	21.48	25.83	22.8
At Fifth line	23.39	24.66	25.95

Typical result showing strain in the x direction ( $\epsilon_{xx}$ ) at three distinct point on the load response of specimen in the pre peak, around peak and in the post peak are shown in Figure 4.12 for 1<sup>st</sup> line located just above the notch, 3<sup>rd</sup> line in the middle of beam and 5<sup>th</sup> line close to the top of the beam and respective loads are tabulated in Table 4.9 for control, 4kg/m<sup>3</sup> and 6g/m<sup>3</sup> specimens. The propagation of crack in the material can be traced from the location of the strain localization. The results clearly indicate that even in the post peak, when the load drops by about 40% of the peak load, the crack does not propagate up to line 5. The strains at line 5 even at load 3 are very small in magnitude and there is no indication of strain localization along the line in Figure 4.13.

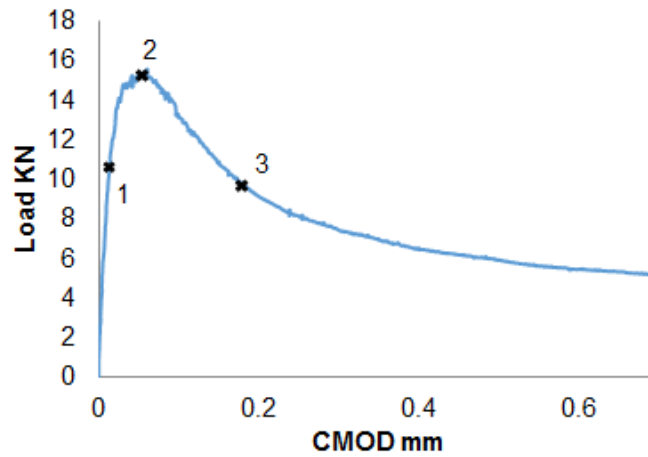
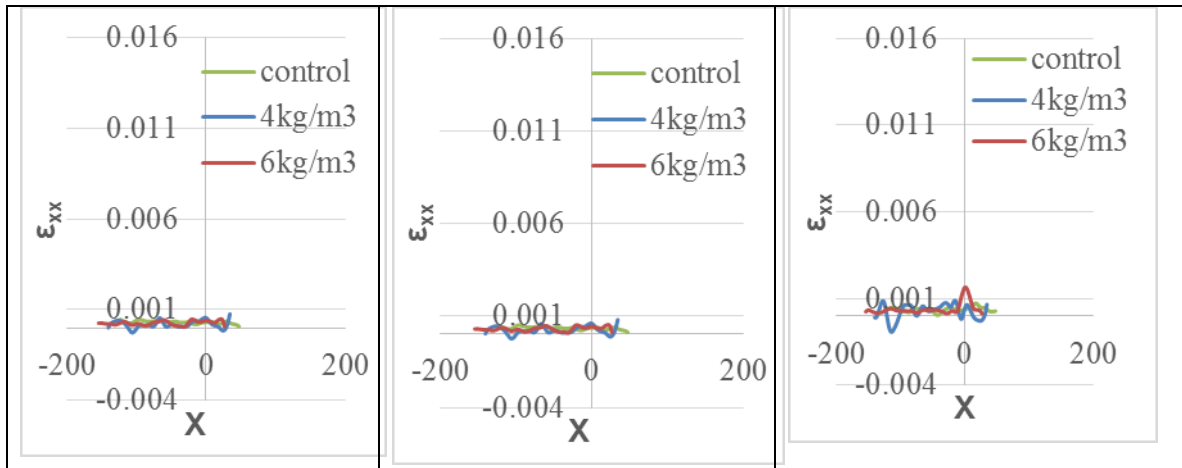


Figure 4.12: distinct point on the load response of specimen at pre peak, around peak and post peak

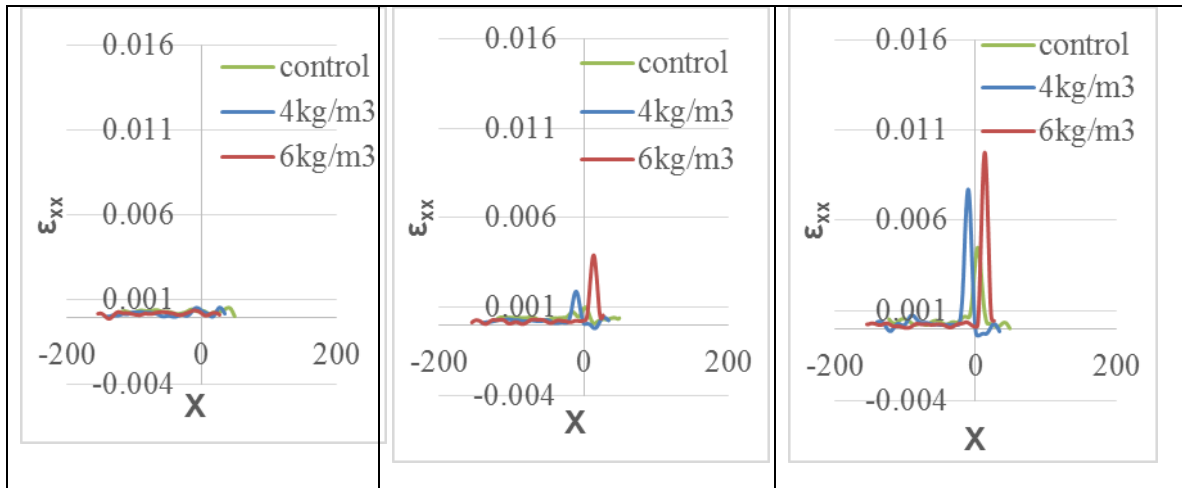




Fifth line – at load 1

Fifth line – at load 2

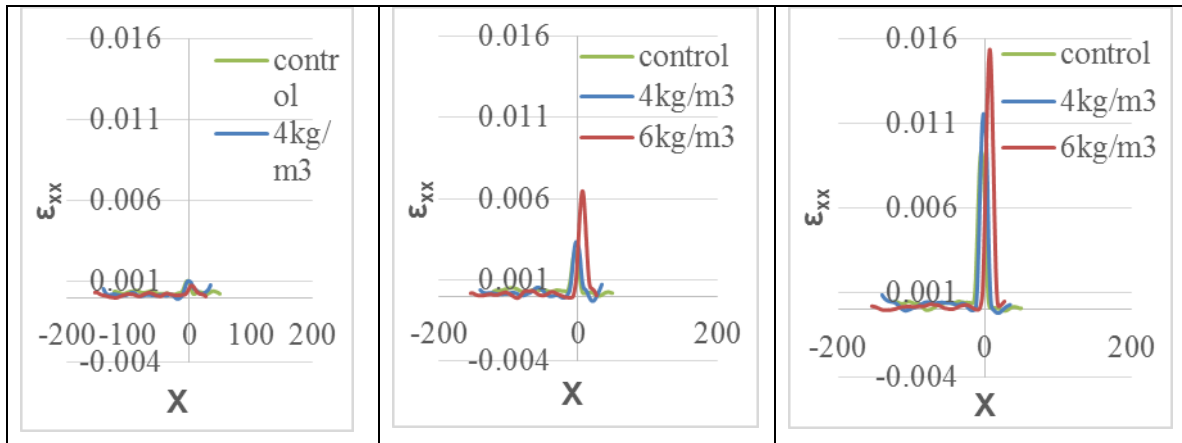
Fifth line – at load 3



Third line – at load 1

Third line - at load 2

Third line – at load 3



First line – at load 1

First line – at load 2

First line – at load 3

**Figure 4.13: Strain at pre peak, around peak and post peak**

Table 4.9: Load at lines

	Control	4kg/m <sup>3</sup>	6kg/m <sup>3</sup>
Load 1	11.3	10.9	10.98
Load 2	15.35	15.1	15.2
Load 3	9.5	10	9.6

#### 4.8 Analysis of Results

The load responses of both notched and unnotched specimens are directly controlled by localization and propagation of a single crack in the cementitious matrix. In the case of notched specimens the notch provides high stress concentration and serves as the originator of the crack. The location of the crack in the specimen is predetermined by the location of the notch. The load response in this case is influenced by the variations in the fracture properties across the depth of the member produced by variations in numbers and embedment lengths of fibers in the plane of crack. In the case of unnotched specimens, the crack forms and propagates at a critical section with inadequate fiber content or low embedment lengths. While the notched specimen does not allow for variations in the fracture properties due to spatial variations in fiber introduced by casting, which would be inherent in real structures, the notched specimen does nevertheless provides information essential to interpreting crack propagation.

The observed load response of SPFRC can be interpreted in terms of crack propagation in the cementitious composite. Comparison of the load deflection response and the corresponding load CMOD response of notched specimens indicates a correspondence between the two responses. The load drop in the post-peak load response is associated with an increase in deflection and CMOD.

A comparison of the CMOD measured during the early part of the load drop in the post-peak response of SPFRC (early part of stage II) is identical to the load drop associated with increasing in CMOD in control specimens. In unreinforced specimens, the post-peak load drop is associated with crack propagation following localization. This indicates that the increase in crack opening displacement, which produces a drop in the load in SPFRC is associated with crack propagation in the cementitious matrix, which is similar to the unreinforced matrix. There is little or no influence of fibers in this stage and the crack continues to propagate in the cementitious matrix. The resistance derived from the fibers

bridging the crack does not produce any significant increase in the crack bridging forces compared to the unreinforced matrix. The deviation from the response of the control specimen after the initial load drop indicates that additional resistance provided by the fibers is noticeable beyond this point, since the crack bridging provided by the aggregate results in steady decrease in the load with increasing CMOD. In the softening part of the load response the resistance derived from the crack bridging forces is clearly lower than the tensile stress released from the matrix when the crack propagates.

At the low volume fractions up to  $4 \text{ kg/m}^3$ , the identical pre-peak and immediate post-peak softening responses from control and SPFRC indicates that the stress transfer to fibers takes place after the formation of the crack. In a composite material, discontinuous random fibers will have different embedment lengths with respect to crack plane. The crack opening is accommodated within fiber slip and elongation. The resistance to crack opening provided by fibers with increasing slip is controlled by debonding and sliding of fibers from the cementitious matrix. Decrease in the load in the post-peak, which results in an increase in CMOD can be interpreted considering the following: (a) the additional capacity provided by the fibers on crack propagation within the range of slip required to accommodate crack opening is smaller than the stress released by the matrix; and (b) the load carrying capacity of the fibers within the range of slip required to produce the required crack opening is decreases with increasing slip. After the load response of SPFRC deviates from the control, the load carried by SPFRC essentially remains constant and even exhibits a slight hardening with increasing CMOD. At this stage there would be significant crack propagation and the additional contribution of fibers with crack advance would be insignificant to the moment capacity. This suggests that the resistance derived from the pullout response of fibers in the existing crack provides sufficient capacity to sustain the load. The hardening load response indicates the likelihood of hardening in the pullout response of the synthetic fiber with increasing slip. Hardening in the pullout-slip response of embossed fibers from a cementitious matrix has previously been reported by Shukla et al [27].

The resistance to crack growth is significantly higher at  $6 \text{ kg/m}^3$ , which is indicated by a deviation from the control response at a lower value of CMOD. Considering the stress transfer to fibers with the propagation of crack in the cementitious matrix, the crack bridging stresses provided by the fibers are sufficient to carry the stress released from the matrix. This happens at a significantly smaller CMOD when compared with  $4 \text{ kg/m}^3$ . This suggests that the crack propagation in the cementitious matrix is influenced at a much smaller crack opening at the higher dosage. The increase in the load with increasing CMOD

suggests that the resistance provided by fibers in the new configuration at increased CMOD is higher than the resistance derived from aggregate and fibers in the older configuration at a smaller CMOD opening (since the resistance from aggregate decreases with increasing crack opening). This indicates a higher resistance to crack growth beyond the threshold load, which would produce a stable crack growth; crack growth occurs only on increasing the load beyond this point. As the crack advances beyond the threshold load, the additional resistance from fibers in the crack advance and the pullout resistance along the existing crack length increase the overall load carrying capacity of the beam.

At  $6\text{kg/m}^3$ , there appears to be a CMOD at which the resistance from fibers is significant to alter the crack propagation in the unreinforced matrix. The role of the fibers is prominent even before the crack arrest load is reached. The exact length of the crack and the CMOD at which the turnaround is achieved would depend upon the stress field in which the crack is located, since this would effect the crack opening profile. Nevertheless the efficacy of fibers can be evaluated by considering the measured CTOD and deflections in a notched beam for a notched beam tested in CMOD control. The crack opening at a deflection of span/150 obtained experimentally is 2.91 mm.

# Chapter 5

## Summary of findings and Future Work

The results of the experimental investigation reveals that at low volume fractions, up to  $6 \text{ kg/m}^3$ , once the matrix has cracked, one of the following types of failure will occur:

At 3 and  $4 \text{ kg/ m}^3$ , the composite may fracture immediately after matrix cracking. This results from inadequate fiber content at the critical section or insufficient fiber lengths to transfer stresses across the matrix crack. Following localization, the crack propagates through the cementitious matrix with little or no resistance from the fibers. The involvement of fibers is seen only at large crack openings.

At  $6 \text{ kg/m}^3$  the composite continues to carry decreasing loads immediately after the peak. The post-cracking resistance is primarily attributed to fiber pull-out. While no significant increase in composite strength is observed, considerable enhancement of the composite fracture energy and toughness is obtained.

The implications of the observed post-peak load carrying ability with fibers are discussed below

The increase in toughness obtained from the use of fibers allows cracks in indeterminate structures to work as hinges and to redistribute loads. In this way, the failure load of the structure may be substantially higher than for the unreinforced structure although the flexural strength of the plain concrete, tested on beams, is not increased.

Polypropylene fibers are not expected to bond chemically in a concrete matrix, but bonding has been shown to occur by mechanical interaction. The elastic modulus of the fiber is 10 GPa while the elastic modulus of mature concrete is expected to be higher than 20 GPa. The effective of the synthetic fibers is expected to be higher at early ages where the improvement in the fracture behavior would be significant relative to cracking load. Synthetic fibers have been shown to be effective in the early lifetime of the composite when

the matrix is itself weak, brittle, and of low modulus. Considering this, macro synthetic fibers have great potential for replacement for shrinkage steel in concrete.

Directions for future research that emerge from the findings of this study are:

1. Investigate larger length of fiber.
2. Investigate the improvements in fracture behavior at early ages.

# References

- [1] R.F. Zollo, Fiber-reinforced concrete: an overview after 30 years of development, *Cem. Concr. Compos.* 19 (1997) 115
- [2] Belletti B, Cerioni R, Meda A, Plizzari G. Design aspects on steel fiber-reinforced concrete pavements. *J Mater Civ Eng* 2008;20(9):599–607.
- [3] Sorelli LG, Meda A, Plizzari GA. Steel fiber concrete slabs on ground: a structural matter. *ACI Struct J* 2006;103(4):551–8
- [4] Ferrara L, Meda A. Relationships between fibre distribution, workability and the mechanical properties of SFRC applied to precast roof elements. *Mater Struct/Mat et Constr* 2006;39(288):411–20
- [5] Gettu R, Barragán B, Garcia T, Ortiz J, Justa R. Fiber concrete tunnel lining. *Concr Int* 2006;28(8):63–9; Bernard E. Correlations in the behaviour of fibre reinforced shotcrete beam and panel specimens. *Mater Struct* 2002;35(3):156–64
- [6] L. Taerwe, A.V. Gysel, *J. Eng. Mech.* 22 (8) (1996) 695–704
- [7] ACI 544.1R-96. (1996) Report on Fiber Reinforced Concrete. American Concrete Institute, Farmington Hills
- [8] ACI 544.3R-93. (1993) Guide for Specifying, Proportioning, Mixing, Placing, and Finishing Steel Fiber Reinforced Concrete. American Concrete Institute, Farmington Hills
- [9] Z. Bayasi, M. McIntyre, *ACI Mater. J.* 99 (4) (2002) 337–344
- [10] Shah and Ouyang, *J. Amer. Cer. Soc.*, 74 (11) 2727-38, 1991
- [11] Johnston, C. D., “Steel Fibre Reinforced Mortar and Concrete—A Review of Mechanical Properties,” *Fiber Reinforced Concrete, SP-44*, American Concrete Institute, Detroit, 1974, pp. 127-142.
- [12] Williamson, G. R., *The Effect of Steel Fibers on the Compressive Strength of Concrete, SP-44: Fiber Reinforced Concrete*, American Concrete Institute, Detroit, 1974, pp. 195-207.
- [13] Johnston, C. D., and Gray, R. J., “Uniaxial Tension Testing of Steel Fibre Reinforced Cementitious Composites,” *Proceedings, International Symposium on*

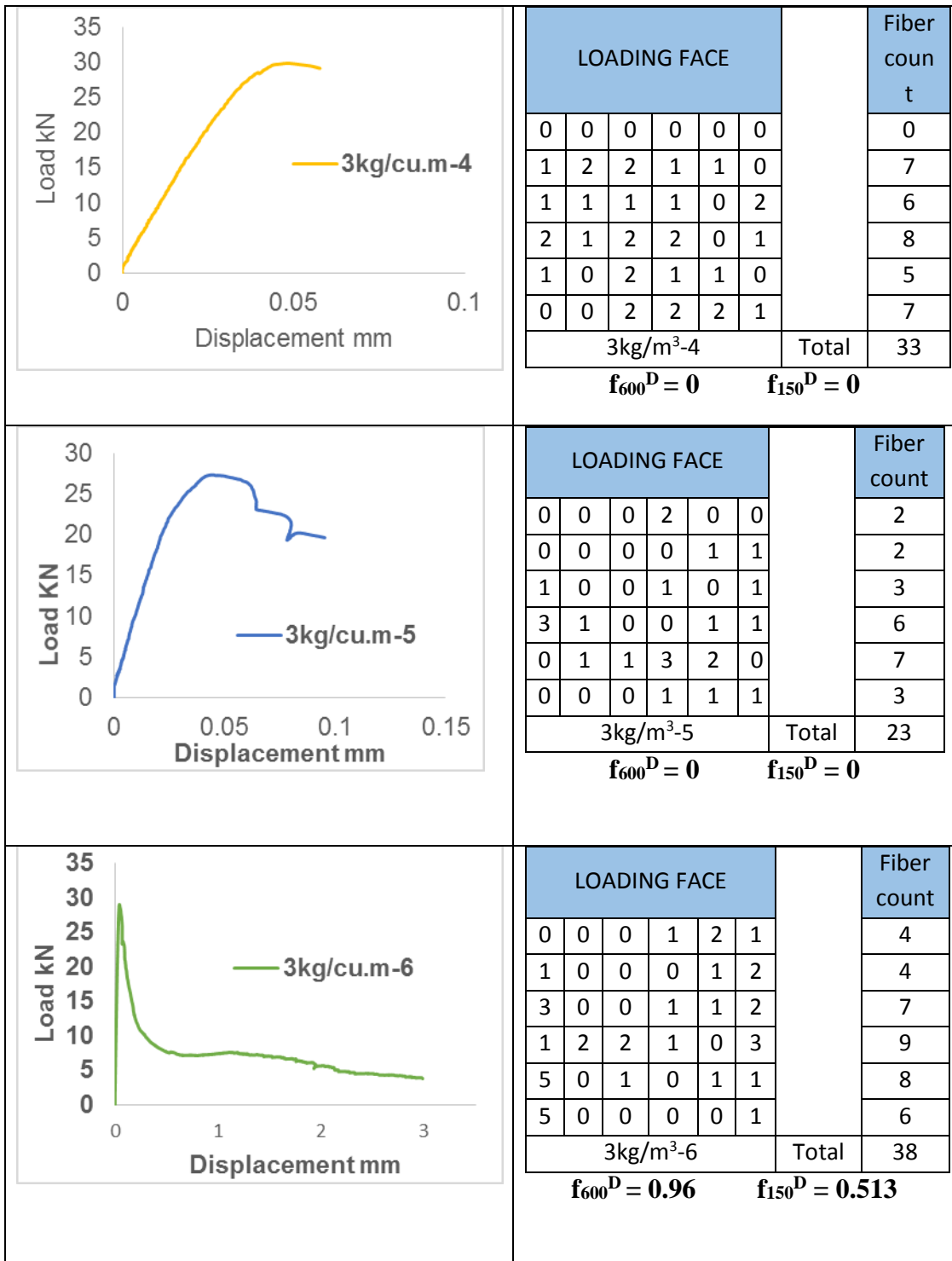
- Testing and Test Methods of Fibre-Cement Composites, RILEM, Sheffield, Apr. 1978, pp. 451-461.
- [14] Kar, N. J., and Pal, A. K., "Strength of Fiber Reinforced Concrete," Journal of the Structural Division, Proceedings, ASCE, Vol. 98, No. ST-5, May 1972, pp. 1053-1068.
- [15] Works, R. H., and Untrauer, R. E., Discussion of "Tensile Strength of Concrete Affected by Uniformly Distributed and Closely Space Short Lengths of Wire Reinforcement," ACI JOURNAL, *Proceedings*, Vol. 61, No. 12, Dec. 1964, pp. 1653-1656
- [16] Johnston, Colin D., and Coleman, Ronald A., "Strength and Deformation of Steel Fiber Reinforced Mortar in Uniaxial Tension," fiber Reinforced Concrete, SP-44, American Concrete Institute, Detroit, 1974, pp. 177-207
- [17] Johnston, C. D., "Definitions and Measurement of Flexural toughness Parameters for Fiber Reinforced Concrete," ASTM, Cement Concrete and Aggregates, Vol. 4, No. 2, Winter 1982, pp. 53-60.
- [18] Brandshaug, T.; Ramakrishnan, V.; Coyle, W. V.; and Schrader, E. K., "A Comparative Evaluation of Concrete Reinforced with Straight Steel Fibers and Collated Fibers with Deformed Ends." Report No. SDSM&T-CBS 7801, South Dakota School of Mines and Technology, Rapid City, May 1978, 52 pp.
- [19] Johnston, C. D., and Gray, R. J., "Flexural Toughness First-Crack Strength of Fibre-Reinforced-Concrete Using ASTM Standard C 1018," Proceedings, Third International Symposium on Developments in Fibre Reinforced Cement Concrete, RILEM, Sheffield, July 1, 1986, Paper No. 5.1
- [20] Hannant, D. J., Fibre Cements and Fibre Concretes, John Wiley & Sons, Ltd., Chichester, United Kingdom, 1978, p. 53.
- [21] H. Cifuentes et al. / Construction and Building Materials 45 (2013) 130–137
- [22] Fracture behavior of concrete members reinforced with structural synthetic fibers by Byung Hwan Oh \*, Ji Cheol Kim, Young Cheol Choi
- [23] Flexural performance of fibre reinforced concrete made with steel and synthetic fibres by M.N. Soutsos, T.T. Le, A.P. Lampropoulos
- [24] Gopalaratnam and Gettu, Cement Concr Compos 1995; 17 (3):239–54

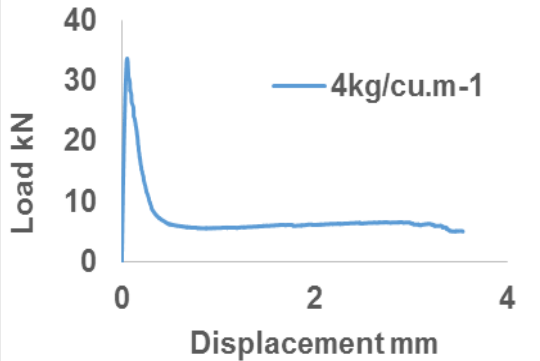
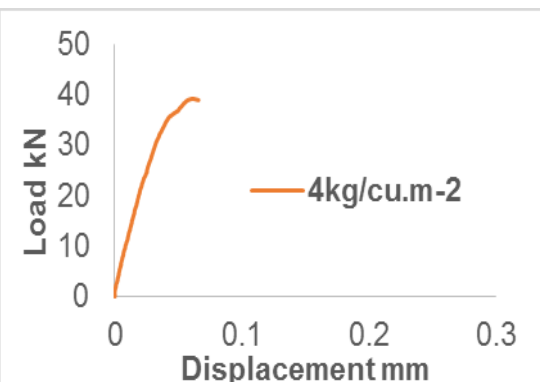
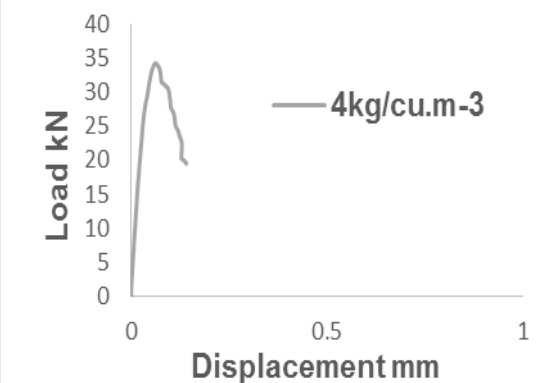


- [25] N.Banathia, J.F.Trottier, Test method of flexural toughness characterization: some concerns and proposition, ACI Material Journal 92 (1) (1995) 48-57.
- [26] Fictitious crack propagation in fiber reinforced concrete beam by J F Olesen
- [27] Pullout behavior of polypropylene fibers from cementitious matrix by Sehaj Singha, Arun Shuklaa,\* , Richard Brownb

# Appendix I

<p>3kg/cu.m-1</p>	<table border="1"> <thead> <tr> <th colspan="6">LOADING FACE</th> <th>Fiber count</th> </tr> </thead> <tbody> <tr><td>2</td><td>0</td><td>1</td><td>1</td><td>1</td><td>1</td><td>6</td></tr> <tr><td>2</td><td>1</td><td>1</td><td>0</td><td>1</td><td>1</td><td>6</td></tr> <tr><td>2</td><td>0</td><td>0</td><td>0</td><td>2</td><td>0</td><td>4</td></tr> <tr><td>2</td><td>3</td><td>0</td><td>0</td><td>1</td><td>0</td><td>6</td></tr> <tr><td>2</td><td>2</td><td>1</td><td>1</td><td>0</td><td>0</td><td>6</td></tr> <tr><td>0</td><td>0</td><td>0</td><td>0</td><td>0</td><td>1</td><td>1</td></tr> <tr> <td colspan="6">3kg/m<sup>3</sup>-1</td> <td>Total</td> <td>29</td> </tr> </tbody> </table>	LOADING FACE						Fiber count	2	0	1	1	1	1	6	2	1	1	0	1	1	6	2	0	0	0	2	0	4	2	3	0	0	1	0	6	2	2	1	1	0	0	6	0	0	0	0	0	1	1	3kg/m <sup>3</sup> -1						Total	29
LOADING FACE						Fiber count																																																				
2	0	1	1	1	1	6																																																				
2	1	1	0	1	1	6																																																				
2	0	0	0	2	0	4																																																				
2	3	0	0	1	0	6																																																				
2	2	1	1	0	0	6																																																				
0	0	0	0	0	1	1																																																				
3kg/m <sup>3</sup> -1						Total	29																																																			
<p><math>f_{600}^D = 0</math>      <math>f_{150}^D = 0</math></p>																																																										
<p>3kg/cu.m-2</p>	<table border="1"> <thead> <tr> <th colspan="6">LOADING FACE</th> <th>Fiber count</th> </tr> </thead> <tbody> <tr><td>2</td><td>3</td><td>6</td><td>0</td><td>1</td><td>0</td><td>12</td></tr> <tr><td>2</td><td>2</td><td>0</td><td>1</td><td>2</td><td>1</td><td>8</td></tr> <tr><td>1</td><td>3</td><td>4</td><td>0</td><td>1</td><td>0</td><td>9</td></tr> <tr><td>2</td><td>1</td><td>0</td><td>1</td><td>2</td><td>0</td><td>6</td></tr> <tr><td>0</td><td>0</td><td>1</td><td>1</td><td>3</td><td>1</td><td>6</td></tr> <tr><td>0</td><td>0</td><td>0</td><td>0</td><td>0</td><td>0</td><td>0</td></tr> <tr> <td colspan="6">3kg/m<sup>3</sup>-2</td> <td>Total</td> <td>41</td> </tr> </tbody> </table>	LOADING FACE						Fiber count	2	3	6	0	1	0	12	2	2	0	1	2	1	8	1	3	4	0	1	0	9	2	1	0	1	2	0	6	0	0	1	1	3	1	6	0	0	0	0	0	0	0	3kg/m <sup>3</sup> -2						Total	41
LOADING FACE						Fiber count																																																				
2	3	6	0	1	0	12																																																				
2	2	0	1	2	1	8																																																				
1	3	4	0	1	0	9																																																				
2	1	0	1	2	0	6																																																				
0	0	1	1	3	1	6																																																				
0	0	0	0	0	0	0																																																				
3kg/m <sup>3</sup> -2						Total	41																																																			
<p><math>f_{600}^D = 0.996</math>      <math>f_{150}^D = 0.663</math></p>																																																										
<p>3kg/cu.m-3</p>	<table border="1"> <thead> <tr> <th colspan="6">LOADING FACE</th> <th>Fiber count</th> </tr> </thead> <tbody> <tr><td>0</td><td>1</td><td>0</td><td>2</td><td>2</td><td>1</td><td>6</td></tr> <tr><td>2</td><td>4</td><td>1</td><td>2</td><td>1</td><td>0</td><td>10</td></tr> <tr><td>2</td><td>1</td><td>1</td><td>2</td><td>6</td><td>2</td><td>14</td></tr> <tr><td>3</td><td>2</td><td>3</td><td>7</td><td>3</td><td>1</td><td>19</td></tr> <tr><td>0</td><td>1</td><td>0</td><td>1</td><td>1</td><td>2</td><td>5</td></tr> <tr><td>2</td><td>1</td><td>0</td><td>0</td><td>1</td><td>1</td><td>5</td></tr> <tr> <td colspan="6">3kg/m<sup>3</sup>-3</td> <td>Total</td> <td>59</td> </tr> </tbody> </table>	LOADING FACE						Fiber count	0	1	0	2	2	1	6	2	4	1	2	1	0	10	2	1	1	2	6	2	14	3	2	3	7	3	1	19	0	1	0	1	1	2	5	2	1	0	0	1	1	5	3kg/m <sup>3</sup> -3						Total	59
LOADING FACE						Fiber count																																																				
0	1	0	2	2	1	6																																																				
2	4	1	2	1	0	10																																																				
2	1	1	2	6	2	14																																																				
3	2	3	7	3	1	19																																																				
0	1	0	1	1	2	5																																																				
2	1	0	0	1	1	5																																																				
3kg/m <sup>3</sup> -3						Total	59																																																			
<p><math>f_{600}^D = 1.168</math>      <math>f_{150}^D = 0.82</math></p>																																																										



 <p>4kg/cu.m-1</p>	<table border="1"> <thead> <tr> <th colspan="6">LOADING FACE</th> <th>Fiber count</th> </tr> </thead> <tbody> <tr><td>0</td><td>1</td><td>1</td><td>1</td><td>2</td><td>2</td><td>7</td></tr> <tr><td>0</td><td>0</td><td>2</td><td>1</td><td>1</td><td>0</td><td>4</td></tr> <tr><td>3</td><td>3</td><td>1</td><td>0</td><td>1</td><td>1</td><td>9</td></tr> <tr><td>1</td><td>0</td><td>3</td><td>2</td><td>4</td><td>1</td><td>11</td></tr> <tr><td>0</td><td>1</td><td>0</td><td>1</td><td>2</td><td>0</td><td>4</td></tr> <tr><td>0</td><td>4</td><td>1</td><td>1</td><td>0</td><td>0</td><td>6</td></tr> <tr> <td colspan="6">4kg/m<sup>3</sup>-1</td> <td>Total</td> <td>41</td> </tr> <tr> <td colspan="6"><b>f<sub>600</sub><sup>D</sup> = 0.75</b></td> <td colspan="2"><b>f<sub>150</sub><sup>D</sup> = 0.844</b></td> </tr> </tbody> </table>	LOADING FACE						Fiber count	0	1	1	1	2	2	7	0	0	2	1	1	0	4	3	3	1	0	1	1	9	1	0	3	2	4	1	11	0	1	0	1	2	0	4	0	4	1	1	0	0	6	4kg/m <sup>3</sup> -1						Total	41	<b>f<sub>600</sub><sup>D</sup> = 0.75</b>						<b>f<sub>150</sub><sup>D</sup> = 0.844</b>	
LOADING FACE						Fiber count																																																												
0	1	1	1	2	2	7																																																												
0	0	2	1	1	0	4																																																												
3	3	1	0	1	1	9																																																												
1	0	3	2	4	1	11																																																												
0	1	0	1	2	0	4																																																												
0	4	1	1	0	0	6																																																												
4kg/m <sup>3</sup> -1						Total	41																																																											
<b>f<sub>600</sub><sup>D</sup> = 0.75</b>						<b>f<sub>150</sub><sup>D</sup> = 0.844</b>																																																												
 <p>4kg/cu.m-2</p>	<table border="1"> <thead> <tr> <th colspan="6">LOADING FACE</th> <th>Fiber count</th> </tr> </thead> <tbody> <tr><td>2</td><td>0</td><td>0</td><td>1</td><td>1</td><td>2</td><td>6</td></tr> <tr><td>0</td><td>1</td><td>0</td><td>0</td><td>2</td><td>1</td><td>4</td></tr> <tr><td>1</td><td>1</td><td>0</td><td>2</td><td>1</td><td>0</td><td>5</td></tr> <tr><td>2</td><td>0</td><td>1</td><td>1</td><td>2</td><td>1</td><td>7</td></tr> <tr><td>1</td><td>2</td><td>3</td><td>0</td><td>1</td><td>1</td><td>8</td></tr> <tr><td>0</td><td>3</td><td>0</td><td>1</td><td>2</td><td>0</td><td>6</td></tr> <tr> <td colspan="6">4kg/m<sup>3</sup>-2</td> <td>Total</td> <td>36</td> </tr> <tr> <td colspan="6"><b>f<sub>600</sub><sup>D</sup> = 0</b></td> <td colspan="2"><b>f<sub>150</sub><sup>D</sup> = 0</b></td> </tr> </tbody> </table>	LOADING FACE						Fiber count	2	0	0	1	1	2	6	0	1	0	0	2	1	4	1	1	0	2	1	0	5	2	0	1	1	2	1	7	1	2	3	0	1	1	8	0	3	0	1	2	0	6	4kg/m <sup>3</sup> -2						Total	36	<b>f<sub>600</sub><sup>D</sup> = 0</b>						<b>f<sub>150</sub><sup>D</sup> = 0</b>	
LOADING FACE						Fiber count																																																												
2	0	0	1	1	2	6																																																												
0	1	0	0	2	1	4																																																												
1	1	0	2	1	0	5																																																												
2	0	1	1	2	1	7																																																												
1	2	3	0	1	1	8																																																												
0	3	0	1	2	0	6																																																												
4kg/m <sup>3</sup> -2						Total	36																																																											
<b>f<sub>600</sub><sup>D</sup> = 0</b>						<b>f<sub>150</sub><sup>D</sup> = 0</b>																																																												
 <p>4kg/cu.m-3</p>	<table border="1"> <thead> <tr> <th colspan="6">LOADING FACE</th> <th>Fiber count</th> </tr> </thead> <tbody> <tr><td>1</td><td>1</td><td>0</td><td>1</td><td>3</td><td>1</td><td>7</td></tr> <tr><td>2</td><td>0</td><td>0</td><td>0</td><td>1</td><td>0</td><td>3</td></tr> <tr><td>0</td><td>0</td><td>1</td><td>1</td><td>1</td><td>1</td><td>4</td></tr> <tr><td>0</td><td>1</td><td>3</td><td>1</td><td>1</td><td>3</td><td>9</td></tr> <tr><td>2</td><td>1</td><td>2</td><td>1</td><td>2</td><td>2</td><td>10</td></tr> <tr><td>2</td><td>3</td><td>1</td><td>0</td><td>1</td><td>1</td><td>8</td></tr> <tr> <td colspan="6">4kg/m<sup>3</sup>-3</td> <td>Total</td> <td>41</td> </tr> <tr> <td colspan="6"><b>f<sub>600</sub><sup>D</sup> = 0</b></td> <td colspan="2"><b>f<sub>150</sub><sup>D</sup> = 0</b></td> </tr> </tbody> </table>	LOADING FACE						Fiber count	1	1	0	1	3	1	7	2	0	0	0	1	0	3	0	0	1	1	1	1	4	0	1	3	1	1	3	9	2	1	2	1	2	2	10	2	3	1	0	1	1	8	4kg/m <sup>3</sup> -3						Total	41	<b>f<sub>600</sub><sup>D</sup> = 0</b>						<b>f<sub>150</sub><sup>D</sup> = 0</b>	
LOADING FACE						Fiber count																																																												
1	1	0	1	3	1	7																																																												
2	0	0	0	1	0	3																																																												
0	0	1	1	1	1	4																																																												
0	1	3	1	1	3	9																																																												
2	1	2	1	2	2	10																																																												
2	3	1	0	1	1	8																																																												
4kg/m <sup>3</sup> -3						Total	41																																																											
<b>f<sub>600</sub><sup>D</sup> = 0</b>						<b>f<sub>150</sub><sup>D</sup> = 0</b>																																																												



